Journal of Vertebrate Paleontology

ISSN: 0272-4634 (Print) 1937-2809 (Online) Journal homepage: www.tandfonline.com/journals/ujvp20

# Coelacanthiform fishes of the British Rhaetian

Jacob G. Quinn, David I. Whiteside, Pablo Toriño, Evangelos R. Matheau-Raven & Michael J. Benton

**To cite this article:** Jacob G. Quinn, David I. Whiteside, Pablo Toriño, Evangelos R. Matheau-Raven & Michael J. Benton (2025) Coelacanthiform fishes of the British Rhaetian, Journal of Vertebrate Paleontology, 45:2, e2520921, DOI: 10.1080/02724634.2025.2520921

**To link to this article:** https://doi.org/10.1080/02724634.2025.2520921

Journal of Vertebrate Paleontology e2520921 (24 pages)
Published with license by the Society of Vertebrate Paleontology
DOI: 10.1080/02724634.2025.2520921



ARTICLE

# COELACANTHIFORM FISHES OF THE BRITISH RHAETIAN

JACOB G. QUINN, [1] DAVID I. WHITESIDE, [1,2] PABLO TORIÑO, [3] EVANGELOS R. MATHEAU-RAVEN,[4]† and MICHAEL J. BENTON [1*,]

[1]School of Earth Sciences, University of Bristol, Bristol BS8 1TF, U.K., xf21604@bristol.ac.uk, David.Whiteside@bristol.ac.uk, mike.benton@bristol.ac.uk;

[2]Fossil Reptiles, Amphibians and Birds Section, The Natural History Museum, Cromwell Road, London SW7 5BD, U.K.;

[3]Instituto de Ciencias Geológicas, Departamento de Paleontología, Facultad de Ciencias, UdelaR, Montevideo, 11.400, Uruguay. Centro Universitario Regional Noreste–sede Tacuarembó, Universidad de la República, Tacuarembó, Uruguay, paleopablo@gmail.com;

[4]131 New Road, Woodston, Peterborough, Cambridgeshire PE2 9HE, U.K., pangaea39@aol.com

ABSTRACT—Coelacanth fishes are well represented in the fossil record, ranging in age from the Early Devonian to the present day, though now represented by only two species of the genus *Latimeria*. After some diversification of form in the Early Devonian, the morphology of coelacanths remained relatively stable throughout the Mesozoic, with distinctive mawsoniid and latimeriid coelacanth morphologies established by the Late Jurassic. Coelacanth remains are well known from Paleozoic and Cretaceous rocks in Britain but poorly known from the Late Triassic. Recently, it was shown that many isolated coelacanth bones from the Rhaetian (latest Triassic) bonebeds had been misidentified as elements of the enigmatic thalattosaur *Pachystropheus rhaeticus*. We further identify a number of coelacanth bones, primarily from the skull, providing descriptions of each for the first time. For some bones, we describe numerous morphotypes, suggesting more than one taxon was present. Most specimens pertain to Mawsoniidae, while others may be assignable to Latimeriidae or are indeterminate coelacanths. We highlight taxonomic misidentifications to show that coelacanth specimens from the British Rhaetian have been confused as far back as the late 1800s. Numerous morphotypes of many bones in the sample hint at a complex community structure, with individuals of varying age, size, and likely several species, supported within the ecosystem. The fossil occurrences suggest these Triassic coelacanths preferred shallow water environments, matching our observation that many specimens pertain to Mawsoniidae, a clade elsewhere reported from brackish, near-shore conditions. In light of recent findings, the new specimens reinforce a European Triassic diversification for Mawsoniidae, which probably influenced their subsequent diversification and dispersion during the Jurassic.

http://zoobank.org/urn:lsid:zoobank.org:pub:56404A79-BF1E-471F-A054-34B54BA8BE51

SUPPLEMENTARY FILES—Supplementary files are available for this article for free at www.tandfonline.com/UJVP.

Citation for this article: Quinn, J. G., Whiteside, D. I., Toriño, P., Matheau-Raven, E. R., & Benton, M. J. (2025) Coelacanthiform fishes of the British Rhaetian. *Journal of Vertebrate Paleontology*. https://doi.org/10.1080/02724634.2025.2520921

Submitted: March 14, 2025
Accepted: June 7, 2025
Revisions received: May 8, 2025
First published online: September 7, 2025

## INTRODUCTION

Coelacanth fishes are known from a range of fossils, as well as two living species of the genus *Latimeria*, the first discovered off the east coast of Africa in 1938, and the second in the western Pacific in 1998 (Clement et al., 2024; Forey, 1998, 2009). After some early divergence in form as the coelacanths split from other osteichthyans in the Early Devonian, the body plan of coelacanths remained relatively stable throughout the Mesozoic, especially from the Late Cretaceous onwards (e.g., Cavin et al., 2021; Clement et al., 2024; Ferrante & Cavin, 2023; Forey, 1998; Friedman & Coates, 2006; Toriño, et al., 2021a). Still, the living *Latimeria* is a popular classic example of a "living fossil" (e.g., Forey, 2009).

Morphological diversity peaked along with increased speciation in the Early Triassic (Cloutier, 1991a, 1991b; Cloutier & Forey, 1991; Forey, 1991, 1998; Toriño et al., 2021a; Wen et al. 2013), though it has been argued that coelacanths displayed little morphological disparity at that time (Schaeffer, 1952). After this peak, coelacanth diversity then declined through the Middle to Late Triassic before stabilizing (Clement et al., 2024; Ferrante & Cavin, 2023). From the Late Triassic to the Late

†Current Address
*Corresponding author.



Color versions of one or more of the figures in the article can be found online at www.tandfonline.com/ujvp.

Cretaceous, the dominant coelacanths were two lineages of Latimerioidae (Cavin et al., 2019, 2021): Latimeriidae, including the extant *Latimeria*, are regarded as marine, deep-water fish, while Mawsoniidae are considered to be brackish or freshwater fish (Cavin et al., 2021; Cupello et al., 2016).

In the U.K., coelacanths are well known from the Paleozoic and Cretaceous (Forey, 1998). Further, coelacanths are prominent in the Triassic of Europe, America, and China (Clement et al., 2024). Despite this rich fossil record, specimens of coelacanths are poorly known in the Late Triassic of Britain, being described from scant and isolated material, including four quadrate bones and a single gular plate of an indeterminate coelacanthiform (Allard et al., 2015; Duffin, 1978:fig. 7; Duffin, 1999: fig. 8; Hauser & Martill, 2013; Moreau et al., 2021). In a recent study of the enigmatic thalattosaur *Pachystropheus rhaeticus*, Quinn et al. (2024) recognized that some appendicular bones and the only cranial element of the reptile had been incorrectly identified, and instead belong to coelacanths. Here we describe these elements, including further materials rediscovered in collections, as well as those previously reported, to create a comprehensive description of all known coelacanth material from the British Rhaetian.

## GEOLOGICAL SETTING

We report specimens from the Rhaetian Westbury Formation (Penarth Group; Fig. 1) and Rhaetian-aged fissure deposits at Holwell, Somerset (Duffin, 1978:fig. 7; Duffin, 1999:fig. 8). The fissure deposits at Holwell are preserved in Neptunian dykes (Robinson, 1957; Weeks et al., 2025; Whiteside & Duffin, 2017), which are sediment-filled fissures that filled by injection during tectonic activity that faulted and jointed the underlying Carboniferous limestone. The infilling of these fissures is thought to have been rapid, with the soft sediment drawn into the tectonically generated fissures as they open, thus dating the age of the infill with the formation of the fissure (Wall & Jenkyns, 2004; Whiteside & Duffin, 2017).

Remains of coelacanths are relatively common in the Westbury Formation, the most basal unit of the Rhaetian Penarth Group (Fig. 1A); extensive outcrops occur around the Bristol Channel, as well as in the English Midlands and Northern Ireland (Fig. 1B; Storrs, 1994). The unit comprises black shales interbedded with siltstones, limestones, and shelly bedding planes varying between 1–15 m in thickness (Storrs et al., 1996). The sedimentology, palynology, and paleontology of the Westbury Formation are well documented (Quinn et al., 2024; Warrington et al., 2008; Whiteside & Marshall, 2008).

Of particular interest are mudstone horizons known as 'Rhaetic Bone beds,' which are interpreted as having been deposited in a shallow, storm-dominated shelf sea (Allington-Jones et al., 2010; Williams et al., 2022). The beds are evidence of the start of extensive and disconformable marine transgression, as well as the end of regional continental deposition in the Triassic (Storrs, 1994; Storrs et al., 1996). The Westbury Formation likely represents quite a short duration (<1 Myr), so despite multiple bone beds and lateral variation between locations, we can treat them as essentially coeval (Williams et al., 2022). The rock sequences are cyclical, suggesting fluctuation in water depth and depositional conditions in marine environments on the continental shelf (Ivimey-Cook, 1974; Larkin et al., 2020; Storrs, 1994). The depth of the water was relatively shallow and poorly circulated, as evidenced by the pyrite in the sediment which is indicative of an anoxic sea floor (Suan et al., 2012); the nearshore conditions in the Late Triassic 'Bristol Archipelago' resulted in high organic and terrestrial iron inputs, that can also be attributed to anoxic conditions (Lovegrove et al., 2021; Storrs, 1994).

Many of the new coelacanth fossils described here occur alongside specimens of *Pachystropheus rhaeticus*, particularly at Garden Cliff, Westbury-on-Severn, Gloucestershire (Fig. 1B, C; Quinn et al., 2024; Williams et al., 2022). Analysis of the paleoecology of *Pachystropheus*-bearing strata revealed a palynomorph assemblage that is dominated by terrestrial spores, with surprisingly few marine dinoflagellate cysts (Quinn et al., 2024). *Ricciisporites tuberculatus* spores were common, which are attributed to *Lepidopteris ottonis*, a wetland plant that became more asexually reproductive, producing an abundance of spores, in response to ecological pressure in stressed environments during the end-Triassic mass extinction (Quinn et al., 2024; Vajda et al., 2023). This suggestion has, however, been rejected by some, based on comparisons of spore ultrastructure (Zavialova, 2024).

## MATERIALS AND METHODS

In a recent study, we noted (Quinn et al., 2024) that several bones previously ascribed to the enigmatic marine reptile *Pachystropheus rhaeticus* in fact belonged to coelacanth fishes. These findings then enabled us to identify other candidate specimens in public repositories. Candidate specimens were tested against a range of possible identities to determine whether they could demonstrably belong to coelacanth fishes or to other taxa. The osteology of coelacanth fish is relatively morphologically conservative through time (Forey, 1998), and there are key differences in the head skeleton between Coelacanthiformes and other osteichthyans, which enabled us to test affinities of the new material against published descriptions and material housed at NHMUK.

We micro-CT scanned NMW 2001.42G.661, NMW 2001.42G.985, and STGCM 1960.62/1 at the μ-VIS X-Ray Imaging Centre at the University of Southampton using the Custom 450/225 kVp Hutch and Modified Nikon/Xtek HMX (225 kVp) tomography scanners using the parameters: 200 kV, 86 uA, 0.02133934 voxel size, 250 ms exposure, and 1 frame per projection. CT data are available on MorphoSource (https://www.morphosource.org/media-lists/000716642?locale=en). We then segmented the scan stack to make a 3D digital model using Dragonfly 3D visualization software (ORS, 2020). In both NMW 2001.42G.985 and STGCM 1960.62, the bone was then manually segmented because the densities of bone and rock were similar, and this enabled the removal of cracks from the scan images. In NMW 2001.42G.661, the high-resolution scan enabled the internal structure of the basisphenoid to be segmented out. This was done in Dragonfly by defining the range in the histogram so that pixels of a light gray color, reflecting where nerve canals in the basisphenoid had become sediment filled or mineralized, were differentiated and could then be interpolated, and converted to a mesh. The data are available on Morphobank (http://morphobank.org/permalink/?P5803).

Finally, we compared the distribution of the 47 new specimens, as well as the three of the known coelacanth specimens (50 total) from the British Rhaetian, to determine whether inferences could be made about their paleoecology based on the geographic spread.

**Institutional Abbreviations—BRLSI**, Bath Royal Literary and Scientific Institution, Bath, U.K.; **BRSMG**, Bristol Museum & Art Gallery, Bristol, U.K.; **BRSUG**, University of Bristol Geology Collection, Bristol, U.K.; **FC-DPV**, Facultad de Ciencias, Departamento de Paleontología, Colección de Vertebrados–UdelaR, Montevideo, Uruguay; **LWL MfN**, LWL-Museum für Naturkunde, Münster, Germany; **NHMUK-PV**, Palaeovertebrate Collection, Natural History Museum, London, U.K.; **NMW**, National Museum of Wales, Cardiff, U.K.; **STGCM**, Museum in the Park, Stroud, U.K.; **WMNM**, LWL-Museum für Naturkunde, Münster, Germany.

## SYSTEMATIC PALEONTOLOGY

In this section, we review all new coelacanth specimens. We identify and separate the remains of mawsoniid and latimeriid

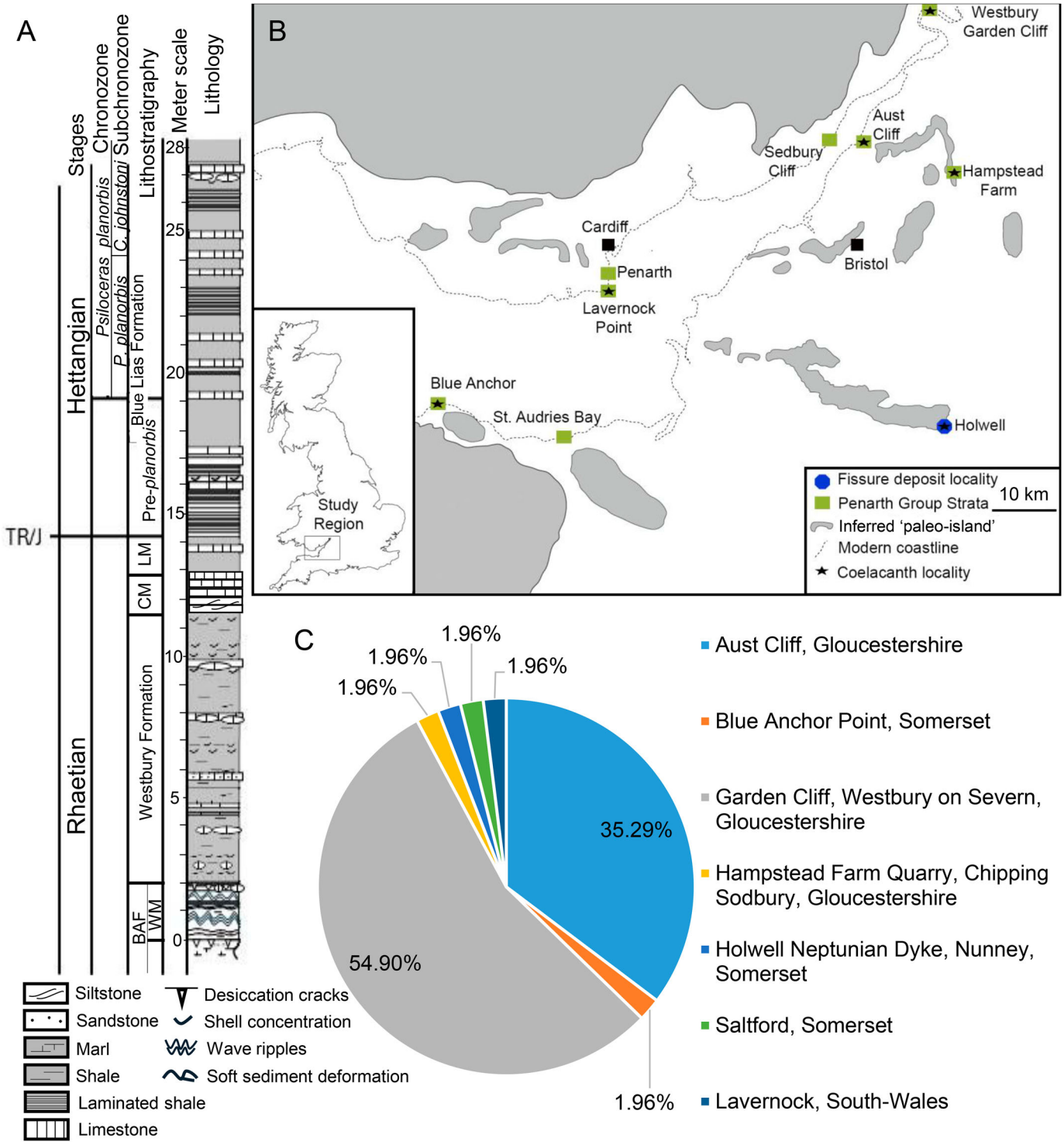


FIGURE 1. **A**, the stratigraphy of the Penarth Group and basal Blue Lias Formation (St Audries Bay, north Somerset). Compiled from Hodges (2021) and Hounslow & Ruffell (2006). **B**, distribution of coelacanth fossils across British Rhaetian localities based on the known specimens, plotted in relation to the inferred paleo-islands. Modified from Lovegrove et al. (2021). **C**, relative distribution of coelacanth specimens (%) against each of the recorded locations. **Abbreviations**: **CM**, Cotham Member (Lilstock Formation); **LM**, Langport Member (Lilstock Formation); **WM**, Williton Member.

taxa by reference to previous research and descriptions of coelacanths. Some ossifications are not character informative, and therefore, are difficult to assign to a specific clade, meaning we consider them as from indeterminate coelacanth taxa.

### Note on the Ossifications of the Coelacanth Skull and Post-Cranial Skeleton

Several bones of the skull of coelacanths are weakly sutured or articulated via cartilage, often occurring as isolated elements in

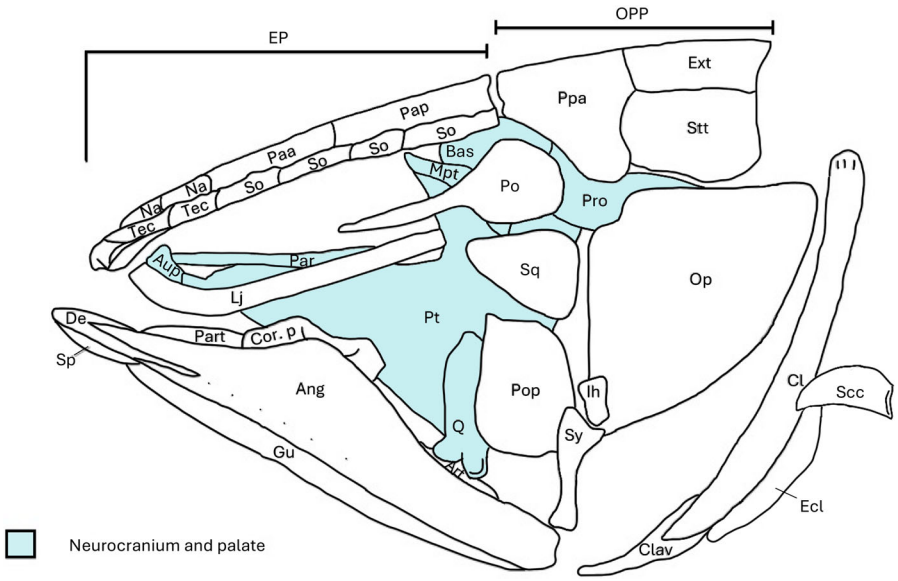


FIGURE 2. Ossifications of a typical mawsoniid coelacanth skull with the addition of the symplectic and interhyal. Neurocranium and palate shaded blue to highlight they are beneath the dermal and exterior bones. Modified from Carvalho (2002). **Abbreviations**: **Ang**, angular; **Art**, articular, **Aup**, autopalatine; **Bas**, basisphenoid; **Cl**, cleithrum; **Clav**, clavicle; **Cor. p**; principal coronoid; **De**, dentary; **Ecl**, extracleithrum; **EP**, ethmosphenoid portion; **Ext**, extrascapulars; **Gu**, gular; **Ih**, interhyal; **Lj**, lachrymojugal; **Mpt**, metapterygoid; **Na**, nasals; **Op**; opercle; **OPP**, otoccipital portion; **Paa**, parietal anterior; **Pap**, parietal posterior; **Par**, parasphenoid; **Part**, perarticular; **Po**, postorbital; **PoP**, preopercle; **Ppa**, post-parietal; **Pro**, prootic; **Pt**, pterygoid; **Q**, quadrate; **Scc**, scapulocoracoid; **So**, supraorbital series; **Sp**, splenial; **Sq**, squamosal; **Stt**, supratemporal; **Sy**, symplectic; **Tec**, tectals.

the fossil record (Forey, 1998). As all the material described here occurs as isolated elements, we give brief descriptions of each region of the skull (Fig. 2), providing context for each of the described ossifications, while highlighting the other bones lacking from our sample that would also comprise each region. Further, a portion of the postcranial skeleton, the shoulder girdle, is briefly described as an area of interest.

**Skull Roof**—The skull roof comprises several dermal bones that cover the dorsal surface of the neurocranium, divided into those anterior and posterior of the intracranial joint (Dutel et al., 2013; Forey, 1998). The parietonasal shield is formed by parietals (frontals, Paa, Pap), nasals (Na), supraorbitals (So), tectals (Tec), rostrals, premaxillae, and preorbitals are regarded as the anterior bones (Fig. 2; Forey, 1998). The postparietal shield is formed by bones posterior to the intracranial joint, namely the postparietals (parietals, Ppa), supratemporals (tabulars, Stt), intertemporals (supratemporals), and extrascapulars (Fig. 2, ex; Dutel et al., 2019; Forey, 1998).

**Neurocranium (Basisphenoid) and Parasphenoid**—The neurocranium of coelacanths is divided into the ethmosphenoid (Fig. 2, EP) and otoccipital regions (OPP), which articulate through the intracranial joint (Dutel et al., 2013; Forey, 1998). Regarding the ossifications of the neurocranium, much is cartilaginous (at least in *Latimeria*), though within the ethmosphenoid, there are both paired lateral ethmoids (ectethmoids) and the basisphenoid (Fig. 2, Bas; Forey, 1998). The ventral surface of the ethmosphenoid is covered by an elongate dermal parasphenoid (Fig. 2, Par; Forey, 1998; Millot and Anthony, 1958).

**Palate**—The palate of coelacanth fishes is characteristic in shape, often considered as triangular (Cloutier, 1991a, 1991b; Forey, 1998). The main ossifications of the coelacanth palate (Fig. 2) include the autopalatine (Aup), pterygoid (Pt), metapterygoid (Mpt), and quadrate (Q; Dutel et al., 2013; Forey, 1998; Manuelli et al., 2024; Toriño, et al., 2021b) while other minor ossifications (dermopalatines and ectopterygoid) are present, but perhaps not in all coelacanths.

**Cheek Bones and Opercula**—In all coelacanths, a well-developed series of bones cover the cheek and opercular region (Forey, 1998). Most of the bones in this region contain a sensory canal. In Latimerioidei (Forey, 1998), the cheek comprises separate elements (Fig. 2), the postorbitals (Po), squamosals (Sq), lachrymojugals (Lj), preopercular (Pop), and opercula (Op; Barbosa et al., 2022; Forey, 1998; Fragoso et al., 2018; Maisey, 1986; Toriño et al., 2021b). The bones in the cheek and opercular region can be highly distinctive among mawsoniid coelacanth species (e.g., *Mawsonia*, Forey, 1998; Toriño et al., 2021b).

**Lower Jaw and Gular Region**—The lower jaws of both fossil and extant coelacanths have been well described and consist of the angular (Ang), dentary (De), splenial (Sp), articular (Art), retroarticular (Art), prearticular (Art), and coronoid (fourth coronoids and principal coronoids, Cor. p; Dutel et al., 2013; Forey, 1998; Toriño et al., 2021b). The mandible is highly apomorphic compared with other teleostomes, exhibiting such characters as large and dorsally expanded angular bones, tandem jaw articulation, and a coronoid series in which the posterior limb projects markedly above the dorsal margin of the angular (Dutel et al., 2013; Forey, 1998).

The gular region lies beneath the lower jaw (Fig. 2) and is marked by two thin and symmetric gular plates (Gu). The gular region of coelacanths has rarely been described (Schultze et al., 2010), although notably shares ornamentation similar to what is seen on the mandible (Barbosa et al., 2022; Forey, 1998; Fragoso et al., 2018; Toriño et al., 2021b).

**Hyoid Arch and Branchial Apparatus**—The hyoid apparatus of coelacanths (Fig. 2) is formed by the hyomandibular, symplectic (Sy), interhyal (Ih), ceratohyal, and hypohyal (Dutel et al., 2013; Forey, 1998). In the branchial apparatus, the main ossifications are represented by the ceratobranchials, which are generally one of the most common elements preserved in the fossil record (Forey, 1998).

**Postcranial Skeleton**—The morphology of the postcranial skeleton is remarkably conservative through time, as well as being highly apomorphic compared with other osteichthyans (Forey, 1998). The postcranial skeleton is divided into the vertebral column (with no ossification of the centra), median fins, shoulder girdle and fins, pelvic girdle and fins, as well as scales (Forey, 1998; Millot & Anthony, 1958, 1965).

Of particular interest is the coelacanth shoulder girdle (Fig. 2), which lies completely free from the skull and includes an extracleithrum (Ecl), a synapomorphy of coelacanths (Forey, 1998). The morphology of coelacanth shoulder girdles is similar in all species, with variations exhibited as minor differences to the cleithrum (Cl) and clavicle (Clav) proportions, and shape of

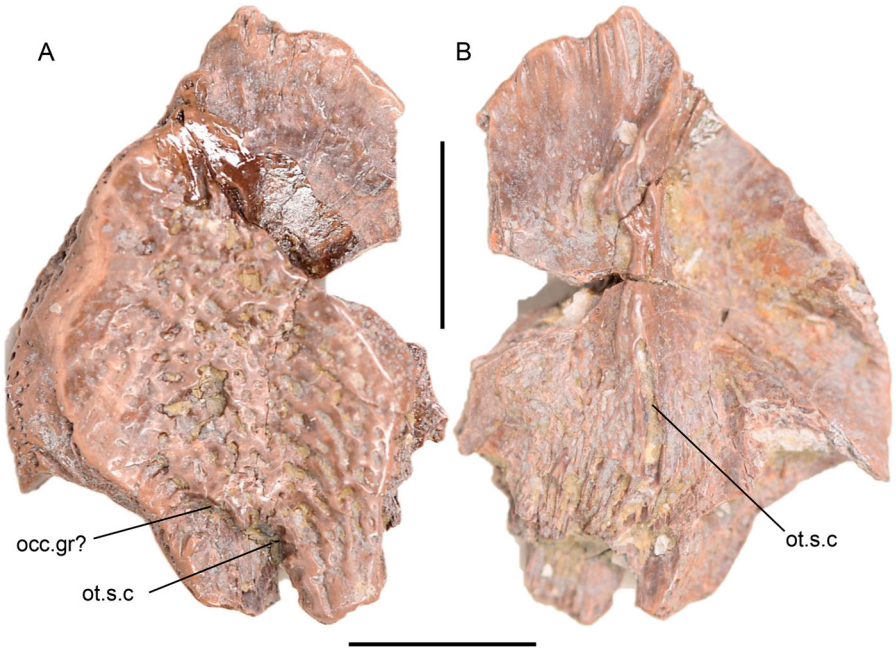


FIGURE 3. Mawsoniid coelacanth skull roof bone. **A**, **B**, BRSMG lot acc. no. 451991 CSB85-82, left supratemporal in dorsal, **A**, and ventral, **B** views. **Abbreviations**: **occ.gr?**, occipital groove; **ot.s.c.**, otic sensory canal. Scale bars represent 10 mm.

anocleithrum (Forey, 1998). The shoulder girdle is usually narrow and made up of an unornamented anocleithrum, extracleithrum, cleithrum, clavicle, scapulocoracoid, and probably a primitive interclavicle (Dutel et al., 2012; Forey, 1998; Mansuit et al., 2020).

SARCOPTERYGII Romer, 1955
ACTINISTIA Cope, 1871
COELACANTHIFORMES Huxley, 1861
LATIMERIOIDEI Schultze, 1993
MAWSONIIDAE Schultze, 1993
MAWSONIIDAE, gen. et sp. indet.
(Figs. 3–11)

Lepidosaurian/Mammalian; Duffin, 1978:61, 63 (quadrate)
*Pachystropheus rhaeticus*; Storrs et al., 1996:329–330, 335–336.
Undetermined coelacanth; Duffin, 1999:218, 221
*Indeterminate coelacanth*; Hauser and Martill, 2013:982–987
*Undetermined coelacanth;* Allard et al., 2015:10, 17, 19, 24, 27–28
Coelacanth sp.*;* Moreau et al., 2021:8, 9; Coelacanthiform; Evans et al., 2024:326–327

**Referred Material**—See Supplementary Files.

**Locality, Horizon, and Age**—Upper Triassic, Rhaetian, Westbury Formation (Penarth Group), from several localities along the Bristol Channel, and Rhaetian-aged Neptunian dyke fissure deposits at Holwell, Somerset.

**Remarks**—Much of the material described here had been previously identified as belonging to other Late Triassic taxa, primarily terrestrial and aquatic tetrapods, found in the same deposits. Further, we reject previous descriptions where material has been misidentified in the literature, such as the coelacanth principal coronoid which was identified as the ectopterygoid of *Pachystropheus rhaeticus* (Sander et al., 2016:fig. 20G; Storrs et al., 1996: fig. 4), demonstrating that such specimens are those of mawsoniid coelacanths. We identify material from the cranial and post-cranial skeleton, including the supratemporal, multiple basisphenoid morphotypes, quadrates, opercula, multiple angular morphotypes, dentary, and principal coronoid from the skull; and clavicle, and neural spine from the post-cranial skeleton. Much of the material exhibits size and characters, such as coarse or rugose external ornamentation and tiny tubercles (though potentially a depositional feature), comparable to a large mawsoniid coelacanth (Dutel et al., 2015a; Toriño et al., 2021b). It is plausible that some of the indeterminate materials described below are mawsoniid in origin, though the bones are uninformative and difficult to diagnose. We find similarities between the material described and the Lower Jurassic mawsoniid *Trachymetopon liassicum* (Dutel et al., 2015a), as well as forms from younger Mesozoic deposits like *Mawsonia* and *Axelrodichthys* (Cavin et al., 2020; Maisey, 1986; Toriño et al., 2021a, b).

## Description

**Skull Roof**—Supratemporal: BRSMG CSB85-82 is identified as a right supratemporal (Fig. 3); it is incomplete, but is a relatively thick bone, and appears to have been tabular shaped (Fig. 3). Despite being incomplete, the preservation of the external and internal surfaces is exquisite. The external surface of the bone is rugose, and ornate with a reticulated pattern and tiny tubercles (Fig. 3A). This ornamented supratemporal is morphologically comparable to the Late Cretaceous *Axelrodichthys megadromos*, which shows the same reticulated ornamentation (Cavin et al., 2020:fig. D2–D3). However, we do also note some similarities in ornamentation with the Early Jurassic mawsoniid *Trachymetopon liassicum* (Dutel et al., 2015a) which is more basal than *Axelrodichthys*. It should be noted that the supratemporal of *Latimeria* is densely pitted on the external surface (Forey, 1998), though the skull roof bones of (Middle) Triassic forms of latimeriids are ornate with denticles (e.g., *Foreyia*; Cavin et al., 2017; and *Tichnepomis*; Ferrante et al., 2023) and not rugosities as seen on BRSMG CSB85-82 (Fig. 3). Unfortunately, BRSMG CSB85-82 cannot be compared with

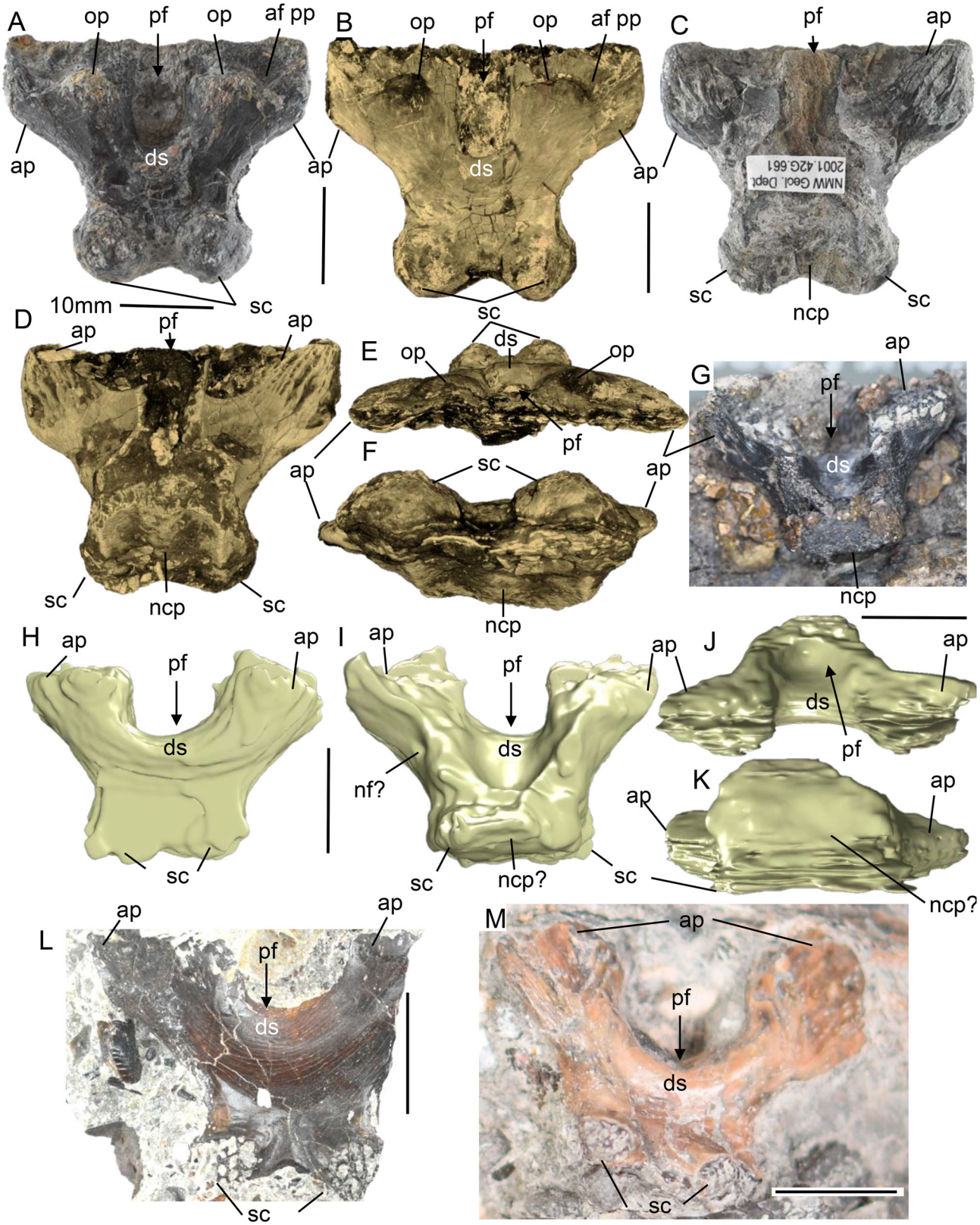


FIGURE 4. Mawsoniid and latimeriid coelacanth basisphenoids. **A**–**F**, NMW 2001.42G.661, morphotype 1, near complete mawsoniid basisphenoid in dorsal **A**, **B**, ventral, **C**, **D**, anterior, **E**, and posterior view, **F**. **A**, **C**, photographs and **B**, **D**-**F**, 3D reconstructions from CT data. **G**–**K**, STGCM.1960.62_1, morphotype 2, partial mawsoniid basisphenoid in ventral, **G**, **I**, dorsal, **H**, anterior, **J**, and posterior, **K,** views. **G**, photograph, and **H**-**K** are 3D reconstructions from CT data. **L**, NMW2020.14G.3, morphotype 2, partial mawsoniid basisphenoid exposed in dorsal view. **M**, BRSMG Cg3102, morphotype 3, partial latimeriid? basisphenoid exposed in dorsal view. **Abbreviations**: **af pp**, articulation facet for the posterior parietal; **ap**, antotic process; **ds**, dorsum sellae; **ncp**, notochordal pit; **nf?**, nutrient foramen; **op**, oval processes; **pf**, pituitary fossa; **sc**, sphenoid condyles. Scale bars represent 10 mm.

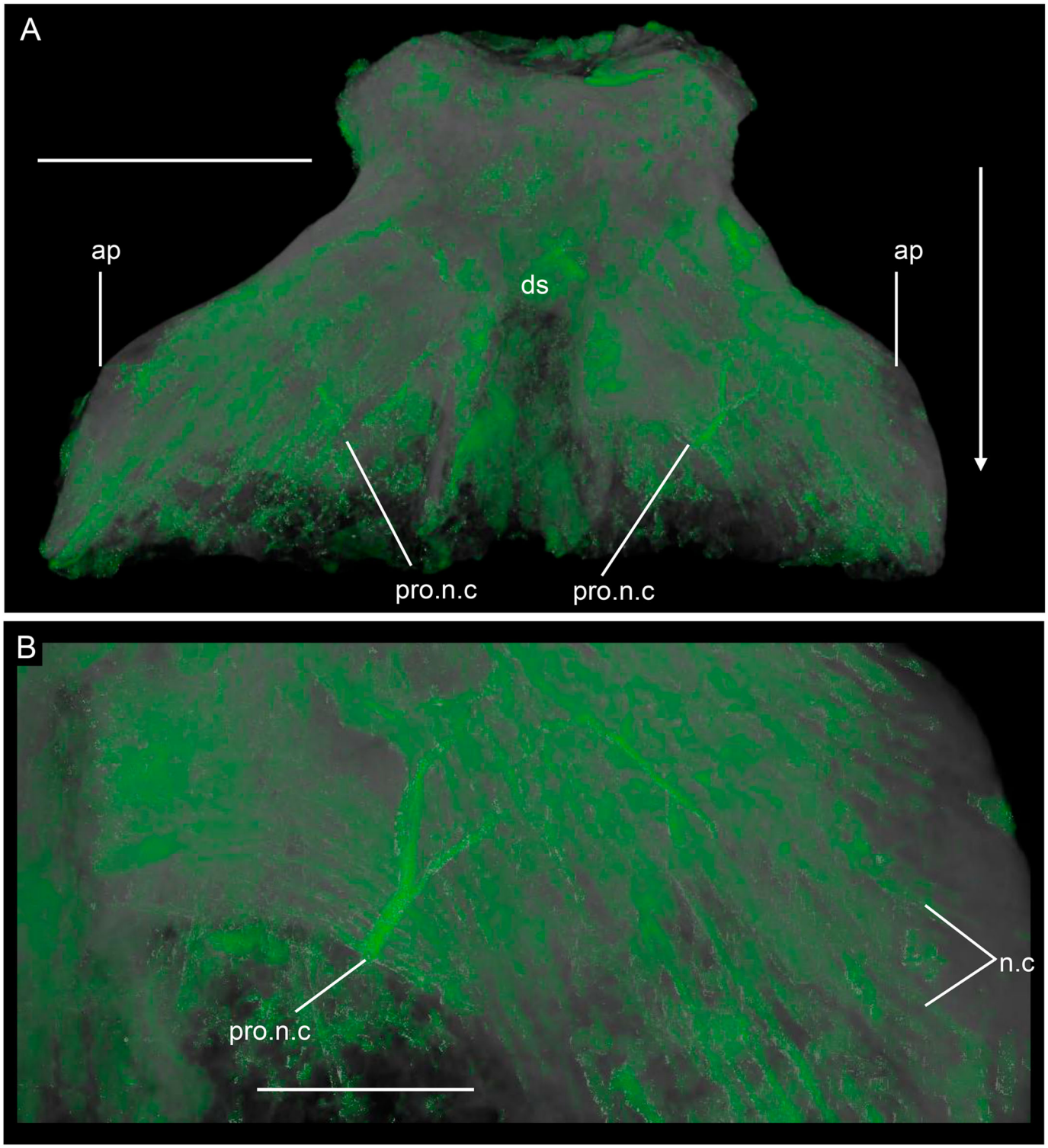


FIGURE 5. **A**, **B**, NMW 2001.42G.661, CT scan of mawsoniid basisphenoid with opacity increased and internal structure segmented to reveal nerve canals and canals for the profundus nerve. **A**, basisphenoid in anterodorsal view; **B**, close-up of the left side of the dorsal surface anterior to the dorsum sellae. **Abbreviations**: **ap**, antotic process; **ds**, dorsum sellae; **n.c**, nerve canal; **pro.n.c**, profundus nerve canal. Scale bars equal 10 mm in **A** and 5 mm in **B**.

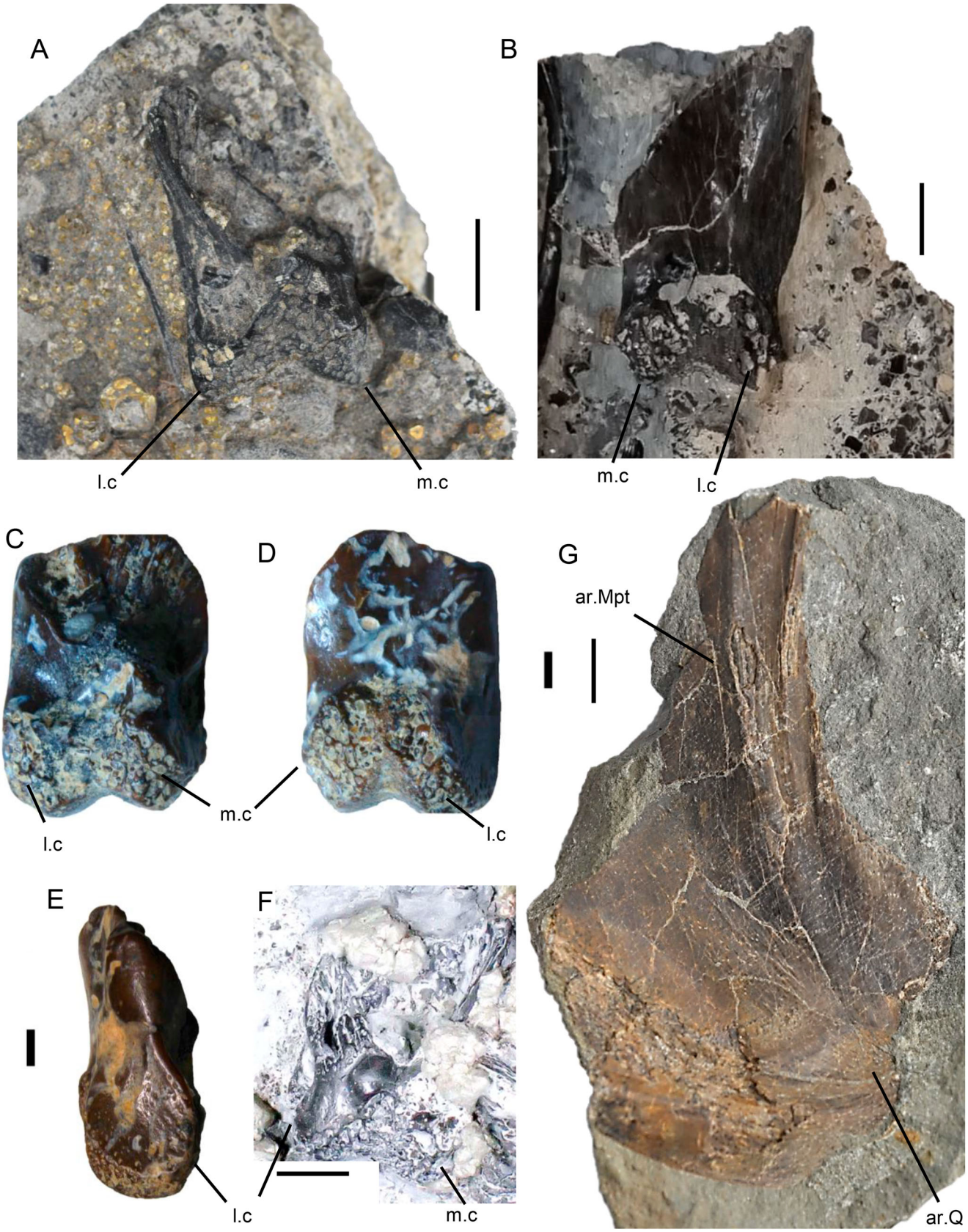


FIGURE 6. Mawsoniid coelacanth palate bones. **A**, BRSUG 25342, morphotype 1, partial left quadrate exposed in posterior view; **B**, NMW 2001.42G.672, morphotype 2, left quadrate exposed in anterior view; **C**–**E**, BRSMG C1, morphotype 1?, left quadrate fragment in posterior, **C**, anterior, **D**, and lateral, **E** views; **F**, NHM PV R 12543, partial left quadrate exposed in posterior view; **G**, NMW2020.14G.4, Mawsoniid right pterygoid in lateral view. **Abbreviations**: **ar.Mpt**, articular surface for the metapterygoid; **ar.Q?**, articular surface for the quadrate; **l.c**, lateral condyle; **m.c**, medial condyle. Scale bars in **A**, **B**, **F**, **G** equal 10 mm, and 1 mm in **C**, **D**, **E**.

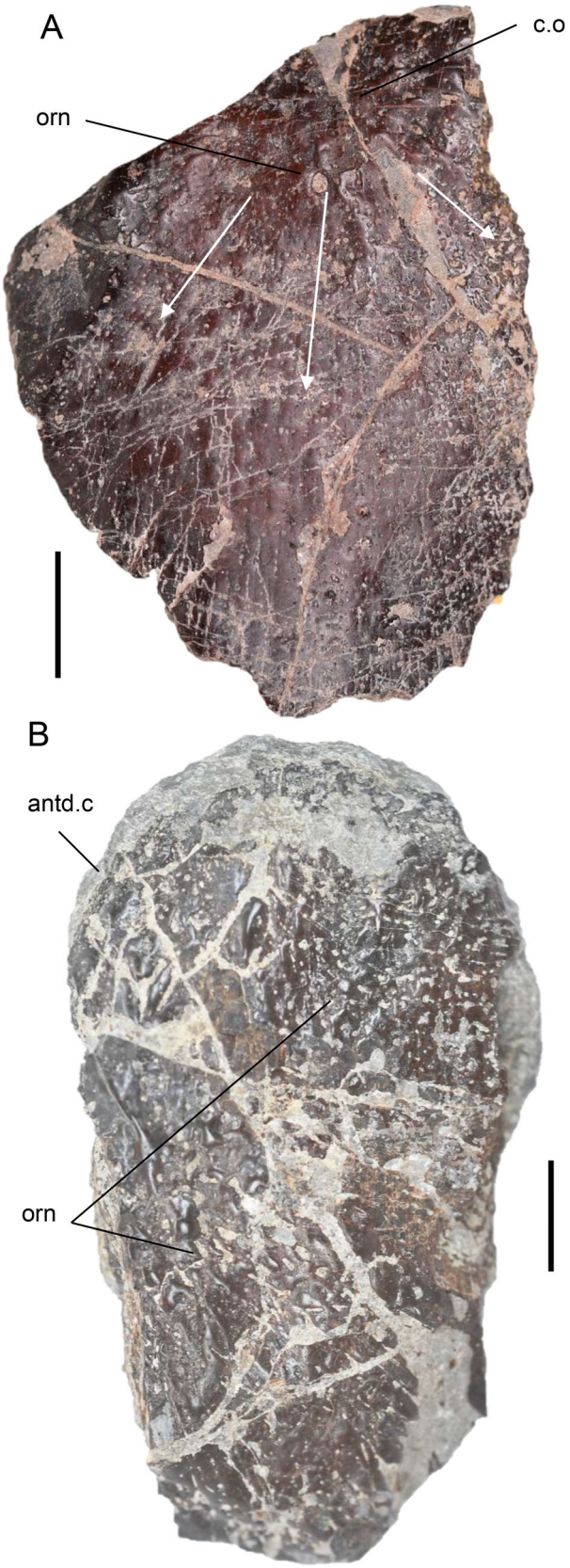


FIGURE 7. Mawsoniid coelacanth opercula. **A**, BRSMG Cf16674, morphotype 1, ?right opercle in lateral view; **B**, NMW2020.14G.6, morphotype 2, ?left opercle in lateral view. White arrows indicate direction of the ornamentation radiation. **Abbreviations**: **antd.c**, anterodorsal corner; **c.o**, center of ossification; **orn**, ornamentation. Scale bars represent 10 mm.

the oldest member of the clade, *Graulia branchiodonta*, as the skull roof bones of the known specimens were damaged during preparation (Manuelli et al., 2024).

The internal surface preserves a sensory canal running anteroposteriorly close to the lateral margin, interpreted here as the otic sensory canal (Fig. 3, ot.s.c; Toriño et al., 2021b:fig. 4). The sensory canal seems superficially more pronounced than in more derived mawsoniid coelacanths (e.g., *Mawsonia*; Toriño et al., 2021b), though this may be due to pre-depositional abrasion to the surface, as part of the sensory canal is exposed. Further, the openings of the sensory canals can be seen where the bone is incomplete. There is a small groove at the posterior of the specimen, but it is unclear whether this is the occipital groove (Fig. 3A, occ.gr; Toriño et al., 2021b:21), as its position with the otic sensory running transversely close to the grove is similar to that of *M. gigas* (Toriño et al., 2021b:fig. 4), or abrasion. It seems that BRSMG CSB85-82 lacks a descending process (Fig. 3), which is usually present in most Latimeriidae and absent in most Mawsoniidae (but not all). For example, in *Axelrodichthys* (Forey, 1998), it is present as a weak ridge, but in the sister genus, *Mawsonia* (Toriño et al., 2021b), it is absent, and both are derived mawsoniids (Schultze, 1993). Although well developed, the ontogenetic stage of the individual is uncertain, as the skull roof bones of coelacanths are well-developed from early ontogenetic stages (Forey, 1998), at least in the only extant coelacanth genus *Latimeria* (Dutel et al., 2019; Millot & Anthony, 1958:pl. 19; Smith, 1940:fig. 3).

**Neurocranium, Parasphenoid, and Vomer**—Basisphenoid: We observe at least two morphotypes of mawsoniid basisphenoid from British Rhaetian deposits. Both morphotypes show the distinctive morphological characters of mawsoniid coelacanths, such as a narrow dorsum sellae and closely spaced, defined sphenoid condyles separated by only a marked notch (Dutel et al., 2015a; Hartung et al., 2021). Morphotype 1, NMW 2001.42.G661, was originally identified as the neural arch of a marine reptile vertebra but instead represents the most complete example of a basisphenoid known from these deposits (Fig. 4A–F). The specimen was dorsoventrally compressed during fossilization but still preserves both the antotic processes and sphenoid condyles (Fig. 4A–F, ap, sc), missing only the ventral surface of the central body. There is a distinct smooth coating of perichondral bone on much of the surface and areas of rough texture that were well cartilage-capped in life (Dutel et al., 2013). The antotic processes are relatively large, extending laterally resulting in a maximum basisphenoid width of 38 mm, compared with its maximum anteroposterior extension of 30 mm, and 7 mm at the dorsoventral maximum. The antotic processes are sub-rectangular in dorsal and ventral views, with the ventral surface bearing strong striations running longitudinally; these striations are articulating surfaces (via cartilage) for the metapterygoids of the palatoquadrate complex (Fig. 4B, C; Maisey, 1986; Toriño et al., 2021b). It should be noted that the ventral surface, albeit not preserved in NMW 2001.42.G661, would have had a similar striated surface for articulation with the posterior end of the parasphenoid (Maisey, 1986; Toriño et al., 2021b). On the dorsal surface, there is a short dorsum sellae (Fig. 4A, B, E, ds) between the antotic processes, adjoined laterally by poorly preserved oval-shaped processes (Fig. 4A, B, E, ds, op). The dorsum sellae merges to become a narrow 'U'-shaped pit, inferred by Hartung et al. (2021) as an extension of the pituitary notch (Fig. 4A, B, pf). In the posterior region, there are two well-developed, spherical sphenoid condyles. Separating the condyles on the ventral side is a slight depression that would sit between the elongated crests of the ventral surface (see Hartung et al., 2021:fig. 4B, G), marking the anterior termination of the notochord (Fig. 4C, D, F, ncp; see Dutel et al., 2013:fig. 3a–e). The sphenoid condyles, along with the processus connectens, affix to the otoccipital division of the braincase (Hartung et al.,

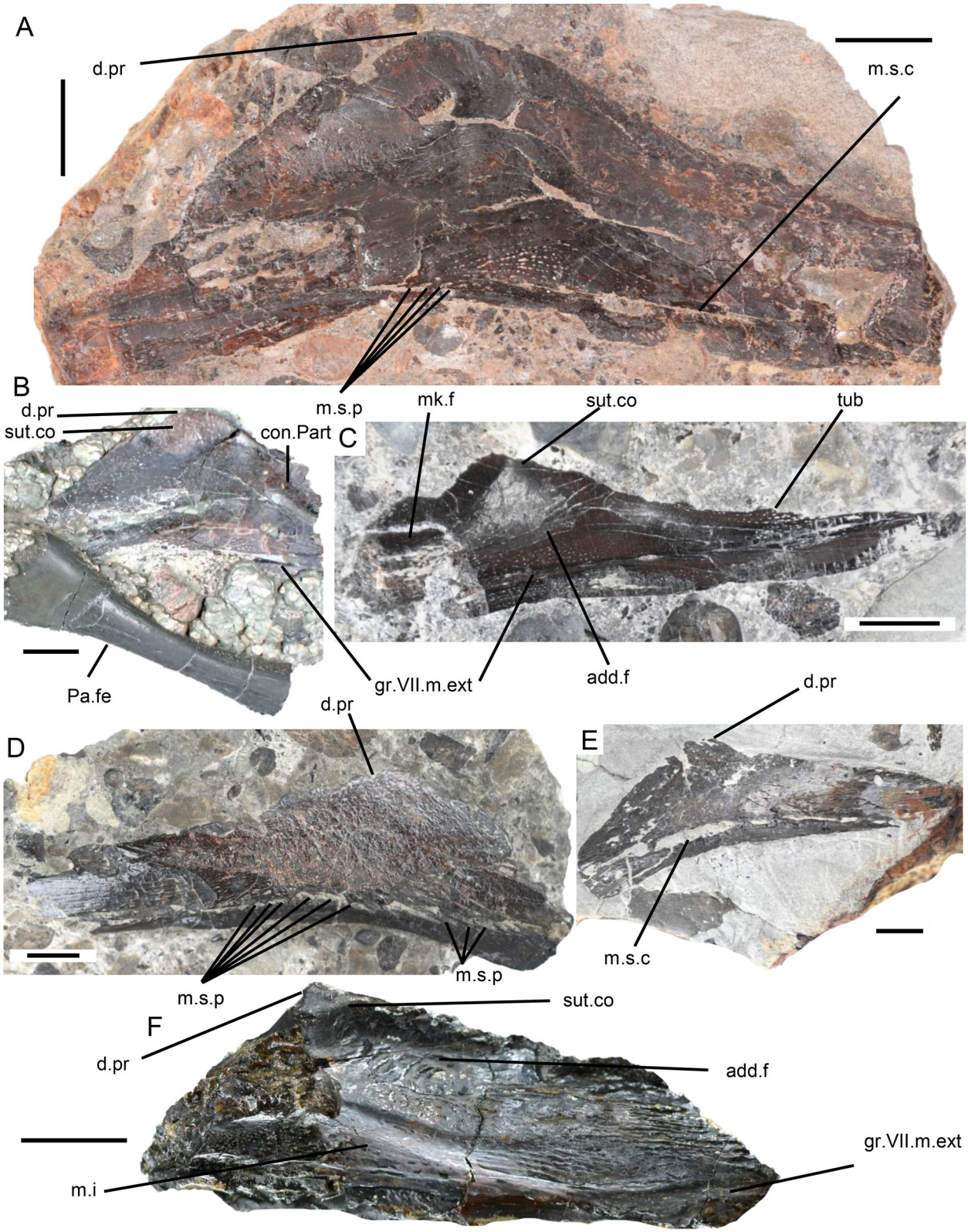


FIGURE 8. Mawsoniid coelacanth angular bones. **A**, BRSMG Ce17375, morphotype 1, partial right angular exposed in lateral view; **B**, NHM PV R 12512, morphotype 1, partial right angular exposed in medial view alongside a *Pachystropheus rhaeticus* femur; **C**, NMW 2001.42G.793, morphotype 2, partial left angular exposed in medial view; **D**, BRSUG 7032.1, morphotype 2, partial left angular in lateral view; **E**, NMW 2001.42G.516, morphotype 2?, partial right angular exposed in lateral view; **F**, NMW2020.1G.1, partial left angular exposed in medial view. **Abbreviations**: **add.f**, adductor fossa; **con.Part**, contact with prearticular; **d.pr**, dorsal process; **gr.VII.m.ext**, groove for external mandibular ramus of facial nerve (VII); **m.i**, medial inflation; **m.s.c**, mandibular sensory canal; **m.s.p**, mandibular sensory pores; **mk.f**, Meckelian fossa; **Pa.fe**, *Pachystropheus rhaeticus* femur; **sut.co**, sutural contact with the principal coronoid; **tub**, tubercles. Scale bars represent 10 mm.

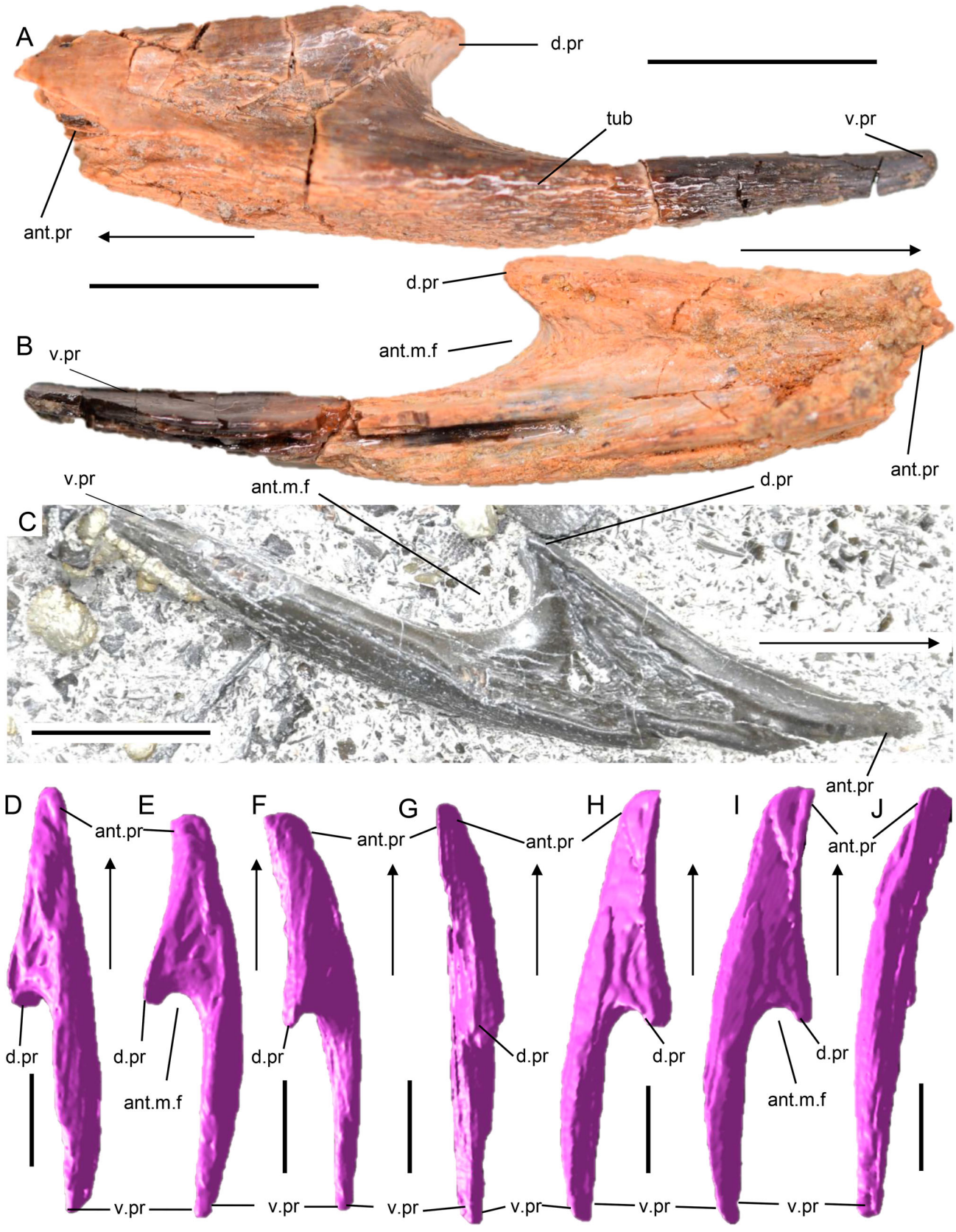


FIGURE 9. Mawsoniid coelacanth dentaries. **A**, **B**, BRSMG lot acc. no. 451991 Cf16006, morphotype 1, partial left dentary lateral, **A**, and medial, **B**, views; **C**–**J**, NMW 2001.42G.985, morphotype 2, right dentary exposed in lateral view, **C**, and 3D reconstruction from CT data in ventrolateral, **D**, lateral, **E**, dorsolateral, **F**, dorsal, **G**, dorsomedial, **H**, medial, **I,** and ventral, **J** views. Arrows indicate the direction of the anterior. **Abbreviations**: **ant.m.f**, anterior part of mandibular fossa; **ant.pr**, anterior process; **d.pr**, dorsal process; **tub**, tubercles; **v.pr**, ventral process. Scale bars represent 10 mm.

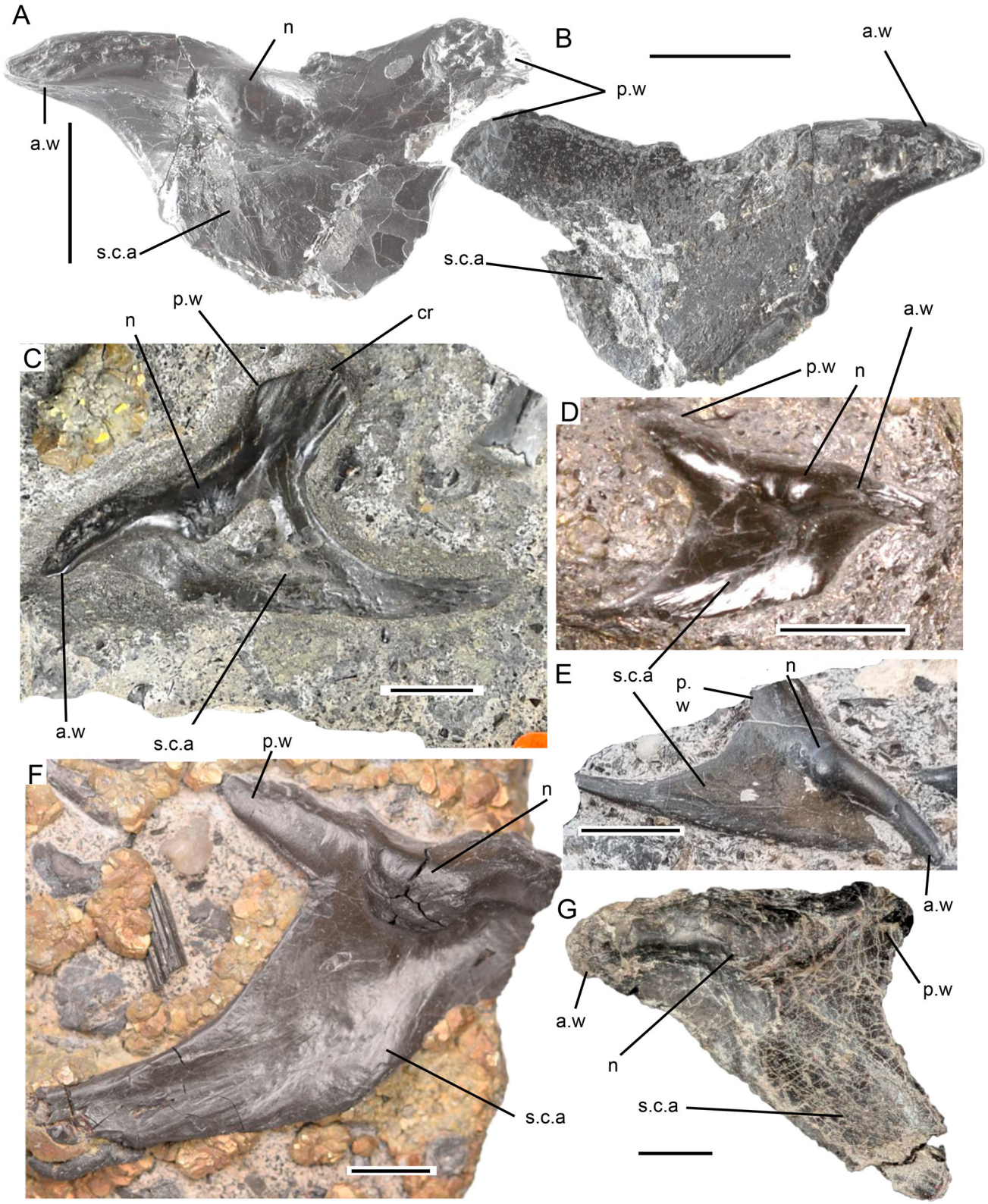


FIGURE 10. Mawsoniid coelacanth principal-coronoid examples, formerly identified as the ectopterygoid of *Pachystropheus rhaeticus* by Storrs et al. (1996). **A**, **B**, BRSUG 25333, morphotype 1, left principal-coronoid of a small individual in lateral, **A**, and medial, **B**, views; **C**, BRSUG 25332, morphotype 2, left principal-coronoid of a large individual exposed in lateral view; **D**, BRSMG lot acc. no. 451991 Cf9543, morphotype 3, right principal-coronoid of a small individual exposed in lateral view; **E**, NHMUK PV R 12510, morphotype 4, right principal-coronoid of a small individual exposed in lateral view; **F**, BRSMG Cd4050, morphotype 5, right principal-coronoid of a large individual exposed in lateral view; **G**, WMNM P97750, morphotype 6, example of a left principal-coronoid of a very large individual from an exposure of 'Rhaetian Bone bed' at Bonenburg, City of Warburg, Kreis Höxter, North Rhine-Westphalia, Germany. **Abbreviations**: **a.w**, anterior wing; **cr**, crenulations; **n**, node; **p.w**, posterior wing; **s.c.a**, sutural contact with angular. Scale bars represent 10 mm.

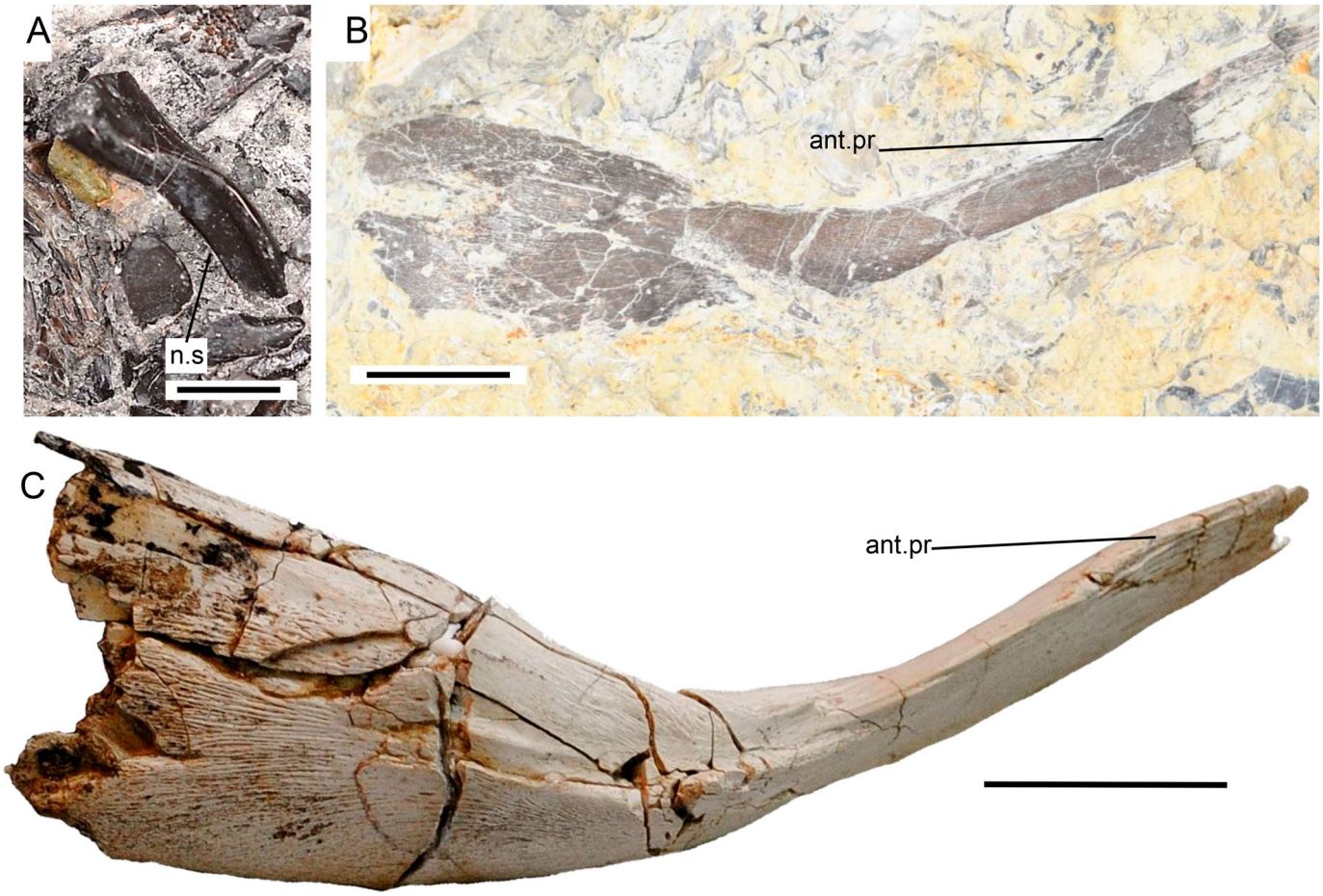


FIGURE 11. Mawsoniid coelacanth bones from the postcranial skeleton. **A**, BRSMG Cg3102, neural spine exposed in lateral view; **B**, NMW2020.14G.7, right clavicle from a large mawsoniid exposed in lateral view; **C**. FC-DPV 2341/2977, right clavicle of *Mawsonia gigas* in lateral view, for comparison. **Abbreviations**: **ant.pr**, anterior process; **n.s**, neural spine. Scale bars equal 10 mm in **A,** and 20 mm in **B** and **C**.

2021; Dutel et al., 2013). There is a rough texture to the sphenoid condyles, indicating it was cartilage capped, which is consistent with the intercranial joints of coelacanths (Fig. 4A, B; Dutel et al., 2013; Hartung et al., 2021:fig. 2A; Toriño et al., 2021b:fig. 7A, F).

CT scans of NMW 2001.42.G661 reveal a hidden network of cranial nerve canals that have mineralized, possibly with pyrite given its abundance throughout the Westbury Formation (Fig. 5). The canal in the basisphenoid begins on the medial surface just anterior to the anterior edge of the dorsum sellae and is identified as a pathway for the profundus nerve (Fig. 5A, B, pro.n.c; Schaeffer & Gregory, 1961). They are paired, appearing on both sides of the dorsum sellae, seemingly branching in different directions posteriorly, although one is only partially preserved. There does not appear to be an exit point, although it is possible this is not preserved. This is similar to modern *Latimeria.* However, it must be noted that the canal for the profundus nerve has also been described in the Early Triassic *Dobrogeria*, a genus close to the divergence of Latimeriidae–Mawsoniidae (Cavin & Grădinaru, 2014), as well as in the Permian *Spermatodus,* in the Lower Triassic *Axelia* and *Wimania* (present before the divergence), and in the latimeriid *Macropoma* (Schaeffer & Gregory, 1961; Stensio, 1921; Watson, 1921), but notably, is absent in the Triassic putative mawsoniid *Moenkopia* (Forey, 1998; Schaeffer & Gregory, 1961).

Morphotype 2, STGCM.1960.62_1 (Fig. 4G–K) and NMW2020.14G.3 (Fig. 4L), show some differences from morphotype 1 and are comparable to WMNM P 81017, a mawsoniid coelacanth basisphenoid described from coeval deposits at the Bonenburg locality in North Rhine-Westphalia, Germany (Fig. 4G–L; Hartung et al., 2021:fig. 3); we thus consider them all the same basisphenoid morphotype. NMW2020.14G.3 is less complete and poorly exposed in the matrix, but the sphenoid condyles are nearly intact. STGCM.1960.62_1 is the more complete of the two specimens, with the antotic processes preserved, but the sphenoid condyles are only partially preserved, and the ventral surface has broken off, likely during transport. Akin to other mawsoniid basisphenoids (Hartung et al., 2021: figs. 2, 3; Toriño et al., 2021b:fig. 7A, F), the antotic processes of STGCM.1960.62/1 are large (though notably less prominent when compared with NMW 2001.42.G66), extending laterally to a maximum basisphenoid width of 32 mm, compared with its maximum anteroposterior extension of 26 mm, and 7 mm at the dorsoventral maximum. In dorsal view, a short dorsum sellae is visible between the antotic processes in STGCM.1960.62/1 and NMW2020.14G.3 but unlike NMW 2001.42.G661 there is no indication of an oval process (Fig. 4B,

op). The processes on both sides of the dorsum sellae of these specimens appear reduced through incomplete ossification or abrasion. As in NMW 2001.42.G661, the dorsum sellae of STGCM.1960.62_1 merge to become a narrow 'U'-shaped pit, thought to be an extension of the pituitary notch (Hartung et al., 2021; Schaeffer & Gregory, 1961). In the posterior of NMW2020.14G.3, there are sphenoid condyles which unlike NMW 2001.42.G661 are ovate not spherical, and are less well-developed and ossified, suggesting this may be from a young individual. There is a shallow depression separating the sphenoid condyles in dorsal view on NMW2020.14G.3, as in NMW 2001.42.G661. CT reconstruction of STGCM.1960.62_1 reveals a single foramen on the ventral surface of the basisphenoid, which may be a nutrient foramen.

Both morphotypes exhibit characters comparable to Mawsoniidae, such as a narrow dorsum sellae and well-defined sphenoid condyles that are separated by a notch (Hartung et al., 2021; Dutel et al., 2015a). The antotic processes are laterally expanded as in basally branching mawsoniids, such as *Chinlea*, *Diplurus*, and *Graulia branchiodonta* (Manuelli et al., 2024; Schaeffer, 1967), but the space between the antotic processes is narrow as in more derived mawsoniids, such as *Axelrodichthys* (Cavin et al., 2020; Fragoso et al., 2019 and *Mawsonia* (Carvalho & Maisey, 2008; Toriño et al., 2021b).

**Palate**—Quadrates: The quadrate is one of two bones described from (juvenile) coelacanths in the Penarth Group, based on three specimens recovered from bonebed sediments from Holwell, Somerset (Duffin, 1999), Manor Farm, Gloucestershire (Allard et al., 2015), and Saltford, Somerset (Moreau et al., 2021), although specimens described by Allard et al. (2015) are fragmentary, and as such, we treat the identification dubiously. Further specimens found at Westbury Garden Cliff, NMW 2001.42G.672 (Fig. 6B) and NHMUK PV R 12543 (Fig. 6F), have now been identified in registered collections, both from considerably larger individuals. All quadrate examples are robust in proportion to their size and like those of mawsoniids (Batista et al., 2019; Torino et al., 2021b). NMW 2001.42G.672 (Fig. 6B) is the most complete and largest of all the specimens. There is a smooth coating of perichondral bone over the surface and areas of rough texture on the inferior extremity, indicating it was cartilage capped (Dutel et al., 2013). In all examples, the superior extremity is largely featureless, but the inferior possesses two distinct condyles. The condyles of the quadrate articulate with the mandible and are stabilized by cartilage and ligaments (Dutel et al., 2013). In most specimens, the lateral and medial condyles (Fig. 6C–E, l.c, m.c) are approximately the same size, as in *Axelrodichthys araripensis* (Fragoso et al., 2018), but differ from BRSUG 25342 (Fig. 6A), where the medial condyle is slightly larger than the lateral. This condition of unequal condyles, the medial larger than the lateral, is seen in coelacanths such as *Mawsonia gigas* (Batista et al., 2019; Carvalho, 2002; Carvalho & Maisey, 2008; Torino et al., 2021b). There is a marked depression on the anterior surface of NMW 2001.42G.672 that extends from the condyles towards the pterygoid. In BRSMG C1 (Fig. 6C–E), the quadrate is narrow and loosely rectangular in shape, as in mawsoniids such as *Mawsonia* (Batista et al., 2019; Torino et al., 2021b). It is notable that, although less robust, this also occurs in latimeriids, including *Megalocoelacanthus dobiei* and the extant *Latimeria* (Dutel et al., 2012, 2013). NMW 2001.42G.672 (Fig. 6B) shows a differing morphology, appearing to curve anteriorly, with a slight constriction near the condyles before expanding laterally towards the pterygoid, as in the Early Jurassic mawsoniid *Trachymetopon liassicum* (Dutel et al., 2015a). The reason for this morphological variation is unknown but may be explained by bone growth during ontogeny or species variation amongst coelacanths in the Penarth Group.

Pterygoid: NMW2020.14G.4 (Fig. 6G), is the only recognized coelacanth pterygoid from the British Rhaetian, exposed in external view. The pterygoid is incomplete, but one of the most distinctively shaped bones of the coelacanth palate (Forey, 1998). This is because the pterygoid is loosely triangular shaped (Cloutier, 1991a, 1991b), extending towards the anterior, very different from that of actinopterygians and other sarcopterygians (Forey, 1998); even so, the shape varies considerably among coelacanth taxa (Forey, 1998:fig. 7.1; Schaeffer & Gregory, 1961:fig. 6). The pterygoid of latimerids is tall (approximately the same height as the length; Dutel et al., 2012; Forey, 1998:fig. 7.2), whereas in mawsoniid coelacanths, it is shallow and elongate (Dutel et al., 2014, 2015; Forey, 1998:fig. 7.1F; Toriño et al., 2024).

Though incomplete, NMW2020.14G.4 is identifiable as the posterior portion of a right pterygoid from a seemingly large individual, with a general morphology referable to Mawsoniidae (see Dutel et al., 2015a:4; Forey, 1998; Maisey, 1986; Manuelli et al., 2024:fig. 22; Toriño et al., 2021b:fig. 8D). At the posterior of the specimen, there is an articular surface for the metapterygoid in the dorsal region (Fig. 6, ar.Mpt), while on the ventral portion there is a small articular surface that is seemingly the articulation for the quadrate (Fig. 6G, ar.Q?) which is seen also in more complete mawsoniid pterygoid examples (e.g., Toriño et al., 2021b:fig. 8D). The posterior margin of the pterygoid looks rounded as in *Mawsonia* (e.g., Maisey, 1986; Toriño et al., 2021b), instead of tending to be straight as in *Latimeria* (e.g., Dutel et al., 2013; Forey, 1998; Manuelli et al., 2024). A ridge, which represents the dorso-ventral ridge of the palatoquadrate, originates dorsally to the quadrate, running anterodorsally to form the anterior margin of the metapterygoid as in *Graulia* (Manuelli et al., 2024:fig. 22) and the Early Jurassic mawsoniid, *Trachymetopon liassicum* (Dutel et al., 2015a:4), and *M. gigas* (Maisey, 1986; Toriño et al., 2021b:fig. 8D). In latimerids, such as *Latimeria* and *Macropoma*, the ventral margin of the pterygoid is swollen (Forey, 1998; Toriño et al., 2021b); though incomplete, the ventral swelling is seemingly absent in NMW2020.14G.4 strengthening the affinity to most Mawsoniidae (except *Axelrodichthys*, which exhibits this character as polymorphic, see Fragoso et al., 2018).

**Cheek Bones and Opercula**—Opercula: We describe just two opercula of differing morphotypes. Both specimens are partial and only the exterior is visible. The specimens are robust and share similar rugosities, which differ from the gracile and tuberculated opercula of the basally branching mawsoniid *Graulia* (Manuelli et al., 2024:14), and are more similar to derived mawsoniids. There are also a number of dermal bones in the BRSMG collections that could be identified as coelacanth opercula, but given that they are fragmentary and could be readily confused with ornamented dermal bones of placodonts, they must be treated as indeterminate.

BRSMG Cf16674 (Fig. 7A) is the only example of opercle morphotype 1. The bone is robust (7 mm thick) and slightly convex, suggesting this is the exterior of the specimen. The exterior surface of the bone has been abraded smooth during deposition, however rugose ornamentation (Fig. 7A, orn) can still be seen radiating from what is likely the central point of the ossification and is reminiscent of derived mawsoniids (Fig. 7A, c.o; Toriño et al., 2021b), although the rugosities are not as well-developed. Akin to most of the bones described here, the opercula are found isolated, but would have been loosely attached to the hyomandibular in life (Forey, 1998). Although only a part of a larger bone, the opercle does not seem to be distinctly triangular shaped as in *Mawsonia* (Toriño et al., 2021b; Forey, 1998) but is more ovate, like that of *Axelrodichthys araipensis* (Forey, 1998:fig. 4.17).

NMW2020.14G.6 (Fig. 7B) is the only example of opercle morphotype 2. The specimen is identified as a left operculum and has

a different morphology to NMW 2001.42G.30. The specimen is more elongate, with a greater ventral extension than in NMW 2001.42G.30; the feature is more similar to *Mawsonia* (Toriño et al., 2021b). The anterior margin of the specimen is straight, but the posterior margin of the specimen is incomplete, so its true shape is unclear. Despite being abraded, the most notable feature of operculum morphotype 2 is the branching rugose ornamentation on the exterior surface (Fig. 7B, orn), seemingly radiating from the anterodorsal corner. The ornamentation is considerably more prominent than in BRSMG Cf16674 and is more similar to the rugose ornamentation seen in *Mawsonia* (Toriño et al., 2021b).

**Lower Jaw and Gular Region**—Angular: Its robust construction means the angular is the most readily recognized coelacanth bone from the British Rhaetian. Indeed, the angular is the most commonly found bone from mawsoniid coelacanths generally, resulting in its use for comparisons between taxa globally (see Cavin et al., 2023:fig. 3). There are numerous examples in collections, most recorded as pieces of bone from an indeterminate reptile, despite their distinct appearance. Angulars are large and robust, with relatively large mandibular sensory canal pores on the lateral surface (Fig. 8A, D, m.s.p), and in some specimens the mandibular sensory canal is exposed where the bone is broken too (Fig. 8A, E, m.s.c). On the medial surface of the angular there is a longitudinal groove which is the groove for external mandibular ramus of the facial nerve (Fig. 8C, F, gr.VII.-m.ext). In all specimens, the anterior and posterior tips are missing (Fig. 8). The medial surface of the angular is concave at the adductor fossa (Fig. 8C, F, add.f). In NMW2020.1G.1 (Fig. 7F), which was misidentified as the anterior tip of a coelacanth gular plate by Evans et al. (2024:fig. 7M), the adductor fossa is markedly more concave than the other specimens and exhibits a faint ornamentation on the medial surface. Further, the medial portion of the bone in NMW2020.1G.1 inflates medially (Fig. 8F, m.i) near to where the sensory canal passes through the bone, similar to *Axelrodichthys* and *Mawsonia* (Forey, 1998:151). Posterior to the adductor fossa, there is a groove which is the Meckelian fossa ('longitudinal fossa' sensu Cavin et al., 2021) (Fig. 8C, mk.f). There is a slight depression on the medial surface of dorsal process (Fig. 8B, F, d.pr) which is the sutural surface for the principal coronoid (Fig. 8B, F, sut.co). In NHMUK PV R 12512, the contact surface for the prearticular is preserved and shows a scalene triangle shape (Fig. 8B, con.Part). On the lateral surface of the angular, relatively large mandibular sensory pores are exposed (Fig. 8A, D; m.s.p), whereas on the medial surface the groove for the external mandibular ramus of the VII nerve can be seen (Cavin & Grădinaru, 2014:fig. 10; Toriño et al., 2021b:fig. 11B). We identify at least two angular morphotypes based on the shape of the dorsal process. Morphotype 1 (Fig. 8A, B) shows greater expansion of the dorsal process, which is rounded at the top near the articulation with the principal coronoid, whereas in morphotype 2, the dorsal process is shallower and more triangular, as in *Mawsonia gigas* (Toriño et al., 2021b) and *Graulia* (Manuelli et al., 2024:fig. 9). The variation in expansion of the dorsal process between morphotypes is also seen in specimens of *Dobrogeria* and has been attributed to ontogenetic variation (Cavin & Grădinaru, 2014: fig. 10), but it is unclear whether this inference is applicable to our sample. The raised hump on the lateral surface of the angular in morphotype 1 (Fig. 8A) is unclear. Many of the angular examples are ornate, with tiny tubercles occurring intermittently on both lateral and medial surfaces (e.g., Fig. 8C, tub), but these might represent pre-burial abrasion. BRSMG 7032.1 is the only angular specimen to exhibit a rugose ornamentation on the exterior surface (Fig. 8D). The rugosity is non-directional, unlike in the angular of derived mawsoniids such as *Mawsonia*, which are ornate with longitudinal rugosity (Cavin et al., 2021; Toriño et al., 2021b). Some other characters related to the deepest point, general outline, sutural contacts, and ornamentation of the angular have been proposed as of taxonomic value for Mawsoniidae. However, these are generally used to differentiate crown sister taxa, such as species of the *Mawsonia–Axelrodichthys* complex (e.g., Forey, 1998; Carvalho & Maisey, 2008; Cavin et al., 2021).

Dentary: The dentary is known from just three specimens, all of which are near complete (Fig. 9). We recognize two morphotypes, each with a characteristic hook shape, but different anterior process. Despite being incomplete, the anterior processes in both morphotypes (Fig. 9, ant.pr) appear as short and slender, before rounding into a point at the apex, similar to the dentaries of the mawsonid *Axelrodichthys* (Cavin et al., 2020), but quite different to *Mawsonia* where there is greater anterior extension (Toriño et al., 2021b, 2022). There are two posterior processes both ventrally and dorsally; the ventral process (Fig. 9, v.pr) articulates with the angular and is elongate, while the dorsal process (Fig. 9, d.pr) articulates with the coronoid 4 and prearticular and is considerably shorter and slenderer (Forey, 1998; Manuelli et al., 2024; Toriño et al., 2021b, 2024). Together the posterior processes form the anterior margin of an elongate mandibular fossa (Fig. 9, ant.m.f), which would be posteriorly bordered by the prearticular and the principal coronoid. All the dentaries studied exhibit a shape characteristic of the *Mawsonia–Axelrodichthys* complex (Forey, 1998). However, neither specimen exhibits the lateral swelling that characterizes some Jurassic and Cretaceous mawsoniid coelacanths (including *Lualabaea*, *Parnaibaia*, *Axelrodichthys*, and *Mawsonia*; Cupello et al., 2016; Forey, 1998; Toriño et al., 2021b, 2022; Yabumoto, 2008). These Rhaetian dentaries are gracile, unlike the more robust dentaries seen in *Mawsonia*, which swell laterally at the mid-length, and those of *Axelrodichthys*, which swell laterally at the anterior margin (Cavin et al., 2021). It is unclear whether lateral swelling is present in more basally branching mawsoniids such as *Graulia* (Manuelli et al., 2024). The lateral swelling may be absent in the dentaries of Late Triassic mawsoniids, just as in the Lower Jurassic mawsoniid *Trachymetopon* (Dutel et al., 2015a; Toriño et al., 2022). Tooth plates may have been attached to the dentaries, but they are loosely attached in extant latimeriids, so, if present in the Rhaetian taxa, they might have separated after death (Manuelli et al., 2024).

Principal coronoid: Originally described as the ectopterygoid of *Pachystropheus* (Sander et al., 2016; Storrs et al., 1996), BRSUG 25333 (Fig. 10A, B), Quinn et al. (2024:fig. 16) reidentified the specimens as the principal coronoid of a coelacanth. There are several examples, all of which are similar, but show some slight variations in morphology and size, giving six morphotypes (Fig. 10). The principal coronoid specimens are saddle shaped, marked by an anterior and posterior wing (Fig. 10, a.w, p.w), the latter of which sits higher in the skull than the anterior, a typical feature of mawsoniid coelacanths, at least in *Axelrodichthys*, *Graulia*, *Mawsonia*, and *Trachymetopon* (Barbosa et al., 2022; Forey, 1998; Fragoso et al., 2018; Manuelli et al., 2025; Toriño et al., 2021b). All specimens are preserved exposing the lateral side only, except BRSUG 25333, which is free from matrix. The medial surface of BRSUG 25333 (Fig. 10B) is abraded and covered by an area of rough texture as in *Graulia* (Maunelli et al., 2024:fig. 9B, D), which is likely the remnants of the shagreen of tiny teeth that would have covered the surface (Forey, 1998). In BRSUG 25332, crenulations (Fig. 10C, cr) can be seen on the lateral surface of the posterior wing. In the middle of the saddle on the lateral surface is a large, bulbous node (Fig. 10A, C–G, n), similar to that of *Mawsoniia* (Toriño et al., 2021b); the node is most prominent in BRSUG 25332, although this may be a reflection of its size, as one of the larger principal coronoids in our sample. In most examples, the sutural contact surface for the dorsal process of the angular is large (Fig. 10, s.c.a), stout at first, but quickly tapers ventrally.

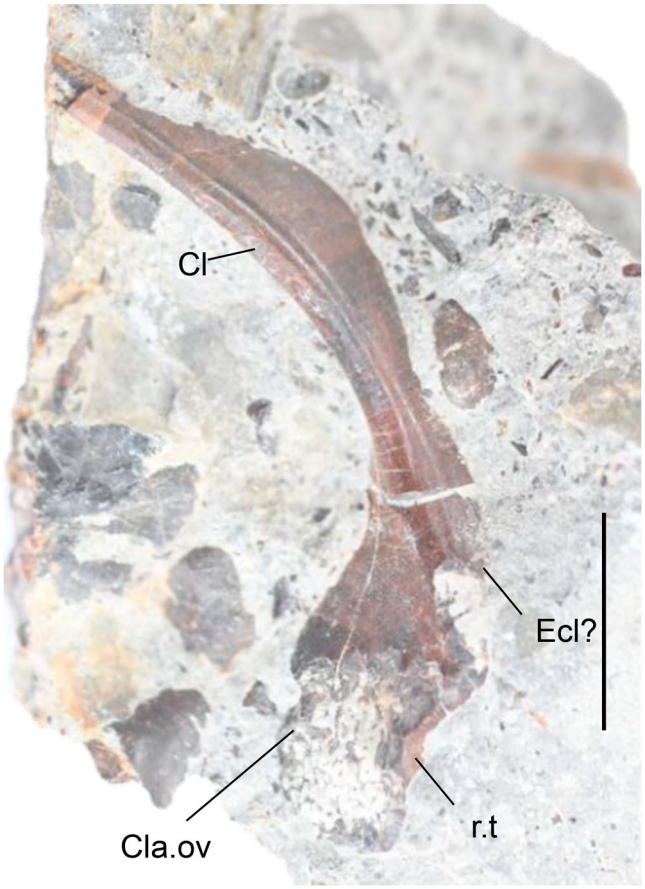


FIGURE 12. Latimeriid? shoulder girdle. NMW2020.14G.8, left cleithrum exposed in lateral view. **Abbreviations**: **Cl**, cleithrum; **Cla.ov**, clavicle overlap surface; **Ecl?**, extracleithrum; **r.t**, rough texture. Scale bar represents 10 mm.

This size of the sutural contact surface for the angular is similar to *Axelrodichthys*, which is described as stout (Cavin et al., 2016; Cupello et al., 2016; Forey, 1998), but differs greatly from *Mawsonia*, where the sutural surface is described as small, or absent (Cavin et al., 2021; Toriño et al., 2021b). Storrs et al. (1996) noted tiny tubercles on the lateral surface of some examples (NHMUK PV R 12510) which conforms with some coelacanth material (Dutel et al., 2015a). Despite the slight variations between the specimens, the principal coronoids are less robust than in *Mawsonia* (Toriño et al., 2021b), appearing as graceful and more like some specimens of *Axelrodichthys* (Barbosa et al., 2022; Cavin et al., 2016; Forey, 1998; Fragoso et al., 2018). It should be noted however, that the graceful appearance of the specimens may be attributed to their overall small sizes.

**Postcranial Skeleton**—Neural spine: The neural spines of fossil coelacanths are poorly described; however, they are short in anterior vertebrae, gradually increasing in length down the vertebral column (Forey, 1998). The ends of the neural spines are cartilage capped in *Latimeria*, although they are also recorded as co-ossified in some fossil examples (e.g., *Trachymetopon*, Dutel et al., 2015a). A partial, isolated neural spine (Fig. 11A, n.s) is identified on BRSMG Cg3102 (Quinn et al., 2024:fig. 3A). The neural spine is laterally compressed (Fig. 11A), with a faint median ridge running parallel along the spine, as in *Trachymetopon* (Dutel et al., 2015a:fig. 2). The distal portion of the neural spine shows moderate lateral expansion but compresses dorsoventrally. The surface of the distal end is rough in texture, suggesting it was cartilage capped as in other coelacanths (Forey, 1998), and may have been a point of articulation for the adjoining elongate neural spine in the medial fin for example (see Dutel et al., 2015a:fig. 2). The example shows moderate curvature towards the distal portion of the neural spine, as in the caudal region of *Trachymetopon*.

Clavicle: The clavicle NMW2020.14G.7 (Fig. 11B) is the second of two post-cranial bones described from a mawsoniid. The specimen is an almost entirely preserved right clavicle with just a small part of the anterior wing missing (Fig. 11B, ant.pr), though fragments and the impression of the missing portion are preserved (Fig. 11B). The specimen is slightly convex and thus preserved in external view; it is assumed the internal surface is concave as in other mawsoniids (e.g., *M. gigas*; Toriño et al., 2021b:figs. 3, 16). NMW2020.14G.7 is the largest of the coelacanth ossifications described here, at 142 mm long. The clavicle is very similar in appearance to that of *Megalocoelacanthus* (Dutel et al., 2012: fig. 18) and *M. gigas* (Fig. 11C; Toriño et al., 2021b:figs. 3, 16; Toriño et al., 2024:figs. 1, 3, and supplementary material therein), bearing a striking resemblance superficially and in size to the latter taxon (Fig. 11C). The body length of FC-DPV 2341/2977 (Fig. 11C) is calculated as between 1.4–1.5 m (Toriño et al., 2024:fig. 6), suggesting a similar size for NMW2020.14G.7, thus evidencing the presence of large-bodied coelacanths in the Rhaetian. Typical for coelacanths, the anterior end twists medially towards the sagittal plane, creating a twisted 'helix' appearance as in *M. gigas* (Toriño et al., 2021b:fig. 16G–J). The posterior end of the clavicle is dorsoventrally expanded, while the anterior is more constricted and graceful, similar to *Mawsonia* and *Axelrodichthys araipensis* (Forey, 1998).

Given that there is limited morphological variation in the shoulder girdles of coelacanths, the right and left clavicles should contact medially via cartilage, in line with the posterior margin of the urohyal (Forey, 1998; Toriño et al., 2021b). The posterior clavicle margin should articulate with the ventral portion of the cleithrum, overlapping part of its lateral face (Dutel et al., 2013; Forey, 1998; Millot & Anthony, 1958). It is unclear how the clavicle proportions compare with the cleithrum, which is unfortunate because the proportions between these bones are diagnostic of certain coelacanth taxa (Forey, 1998).

LATIMERIIDAE Berg, 1940 sensu Dutel et al., 2012
LATIMERIIDAE?, gen. et sp. indet.
(Figs. 4, 12)

**Referred Material**—See Supplementary Files.

**Locality, Horizon, and Age**—Upper Triassic, Rhaetian, Westbury Formation (Penarth Group), from several localities around the Bristol Channel.

**Remarks**—We identify material from the cranial and post-cranial skeleton, which includes a basisphenoid and cleithrum. We demonstrate that such elements are morphologically distinct from mawsoniids and instead likely belong to latimeriid coelacanths, although the relationships among early-diverging latimerioid coelacanths are unclear, and diagnostic characters vary between samples. Some of the indeterminate bones described later might be latimeriid, though the bones are uninformative and so difficult to diagnose. We find similarities between the new materials and latimeriids such as *Ticinepomis* (Cavin et al., 2013; Ferrante et al., 2023), *Megalocoelacanthus* and *Latimeria* (Dutel et al., 2012:fig. 15B; Dutel et al., 2013:fig. 1A).

## Description

**Neurocranium, Parasphenoid, and Vomer**—Basisphenoid: A third basisphenoid morphotype is also reported on BRSMG Cg3102 but the specimen is exposed dorsally only and attempts

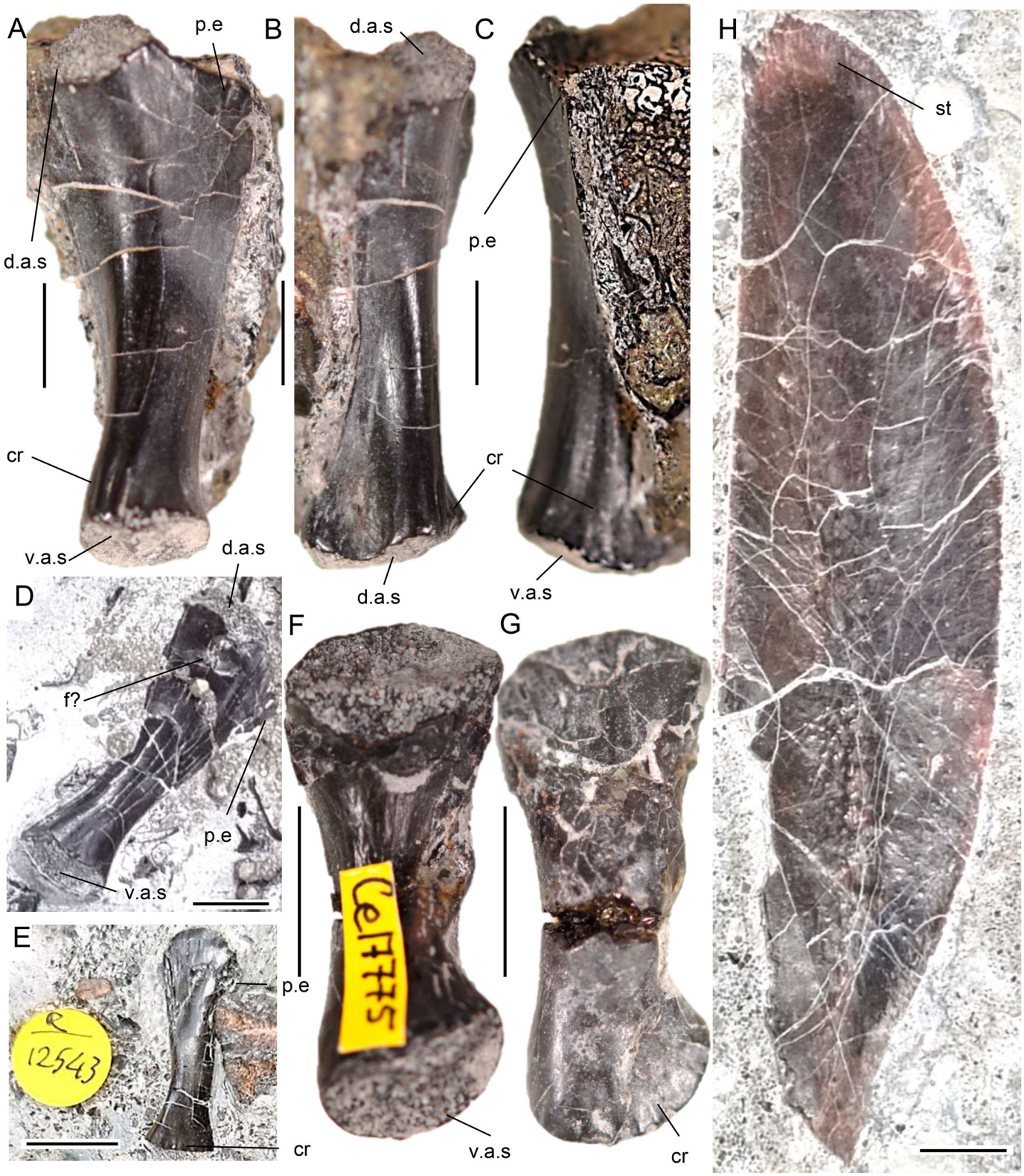


FIGURE 13. Indeterminate coelacanth bones. **A**–**C**, BRSMG Ce17773, morphotype 1, left symplectic in lateral, **A**, anterior, **B**, and posterior, **C** views; **D**, NHM PV R 12480, morphotype 1, right symplectic exposed in medial view; **E**, NHM PV R 12543, morphotype 2, ?left symplectic exposed in lateral view; **F**–**G**, BRSMG Ce17775, morphotype 3, left symplectic in medial, **F**, and lateral, **G** views; **H**, NHM PV P 73214, right gular plate from a large indeterminate coelacanth exposed in dorsal view. **Abbreviations**: **cr**, crenulations; **d.a.s**, dorsal articular surface; **f?**, foramen; **p.e**, posterior extension; **st**, striae; **v.a.s**, ventral articular surface. Scale bars represent 10 mm.

to CT scan the rock failed because the slab is too thick (Fig. 4M). Although we note some slight deformation to the specimen, morphotype 3 differs from those identified as mawsoniid basisphenoids, showing less prominent sphenoid condyles that are separated by a wider gap, and a comparatively wide dorsum sellae also (Deesri et al., 2018; Dutel et al., 2012; Hartung et al., 2021), similar to *Latimeria chalumnae* (Forey et al., 1985; Forey, 1998), but most similar to *Macropoma lewesiensis* (Forey, 1998: fig. 6.12B), thus supporting the affinity to Latimeriidae. Similarly to morphotypes 1 and 2, BRSMG Cg3102 (Fig. 4M) preserves the antotic processes, dorsum sellae, and sphenoid condyles, but there are some morphological differences. Anteriorly (Fig. 4M), the antotic processes extend laterally, as in *M. lewesiensis* (Forey, 1998:fig. 6.12B), and are not as large as in mawsoniid basisphenoids (Fig. 4A–L; Hartung et al., 2021:fig. 2, 3; Toriño et al., 2021b:fig. 7A, F). Further, the antotic processes of BRSMG Cg3102 (Fig. 4M) appear obovate in shape and are less prominent than in both morphotypes 1 and 2 (Fig. 4A–L). There is a short dorsum sellae visible between the antotic processes. Similarly to morphotype 2, there are no indications of the oval processes associated with the dorsum sellae (noted in morphotype 1) preserved in BRSMG Cg3102; the basisphenoid is well-preserved and such processes appear to be completely absent, conversely to morphotype 2, where it is suggested that these oval processes on both sides of the dorsum sellae were lost through depositional abrasion. As in both other basisphenoid morphotypes, the dorsum sellae of BRSMG Cg3102 merges to become a 'U'-shaped pit, thought to be an extension of the pituitary notch (Hartung et al., 2021; Schaeffer & Gregory, 1961), but the pit is relatively wide rather than narrow as in morphotypes 1 and 2. In the posterior of BRSMG Cg3102 there are sphenoid condyles; similarly to morphotype 1, the condyles are spherical, but are smaller and less well-ossified. There is a shallow depression separating the sphenoid condyles as in other basisphenoid morphotypes.

**Postcranial Skeleton**—Cleithrum: NMW2020.14G.8 is identified as the cleithrum from the shoulder girdle of a latimeriid coelacanth (Fig. 12, Cl). The specimen appears mostly complete and preserved in lateral view, but obscured by the surrounding matrix. It is overall well-ossified, but could be from a juvenile or small adult individual, comparing well to both ontogenetic stages in *Latimeria chalumnae* (Mansuit et al., 2020:fig. 3). The cleithrum is relatively slender, extending dorsoventrally and presents a moderate curvature towards the anterior of the bone, though not as strong as in mawsoniids (e.g., *Mawsonia*; Toriño et al., 2021b). The specimen looks laterally compressed, exhibiting a lateral swelling in the medial portion of the bone, similar to *Megalocoelacanthus* (Dutel et al., 2012). There is a marked depression directly below the curvature of the bone in the posterior of the ventral portion of the cleithrum, becoming weaker dorsally, which is interpreted as the point of articulation for the extracleithrum (Fig. 12, Ecl?), as in *L. chalumnae* and *Megalocoelacanthus* (Dutel et al., 2012; Mansuit et al., 2020). Though generally well-ossified, there is an area of rough texture on the ventral portion (Fig. 12, r.t), but it is unclear whether this portion of the bone was cartilaginous where overlapped by the clavicle (Fig. 12, Cla.ov) or this represents postmortem damage. Unfortunately, the medial face of the cleithrum is obscured by rock, and so the articulation points for the anocleithrum (dorsal end) and scapulocoracoid cannot be seen, assuming it is similar to other coelacanths (Forey, 1998; Mansuit et al., 2020; Toriño et al., 2021b).

## Family, genus, and species indeterminate (Fig. 13)

*Pachystropheus rhaeticus*; Storrs et al., 1996:329–330, 335–336
*Indeterminate coelacanth*; Hauser and Martill, 2013:982–987
*Pachystropheus rhaeticus*; Williams et al., 2022:11, 13

**Referred Material**—BRSMG Cg3102; NMW2020.14G.8.

**Locality, Horizon, and Age**—Upper Triassic, Rhaetian, Westbury Formation (Penarth Group), from several localities around the Bristol Channel.

**Remarks**—Similarly to the mawsoniid specimens described earlier, some of the material had previously been assigned to marine tetrapods. Both symplectic morphotypes from the hyoid arch had previously been identified as bones of the marine reptile *Pachystropheus rhaeticus*, with one figured as the left caudal rib (Storrs et al., 1996:fig. 6B) and the other as an epipodial (Williams et al., 2022:fig. 10f). It is plausible that some of the materials described originate from latimerioid coelacanths, although the bones are uninformative and so difficult to diagnose, meaning they should be treated as indeterminate.

### Description

**Hyoid Arch**—Symplectic: The symplectic, BRSMG Ce17773 (Fig. 13A–C), was originally identified as belonging to the enigmatic marine reptile *Pachystropheus rhaeticus* (Williams et al., 2022) but was later shown to be the symplectic of a coelacanth (Quinn et al., 2024:fig. 16). Symplectic bones are usually briefly defined in descriptions of coelacanths, but the specimen is well preserved showing great detail. The shape of the symplectic is typical of other latimerioid coelacanths, with an upper part enlarged posteriorly to form a hatchet shape (Fig. 13A, C, p.e; Dutel et al., 2012, 2015b; Manuelli et al., 2024:figs. 5C, 12E). The dorsal portion is more enlarged than the ventral and crenulations (Fig. 13A–C, cr) can be seen ventrally running up the base of the robust shaft that appears twisted in lateral view (Fig. 13B). Both dorsal and ventral ends are marked by a rough texture, indicating the bone was well-capped with cartilage, and the actual length may have been longer, as in other coelacanths (Dutel et al., 2012, 2015b; Forey, 1998). On the medial surface of NHM PV R 12480 there is a circular depression that may be a foramen (Fig. 13D, f?). NHMUK PV R 12543 shares these characters too, but the dorsal end differs in that it is more rounded, with less posterior extension (Fig. 13E). Overall, the specimens described are very similar and morphologically comparable to the symplectic bones of the Middle Triassic *Graulia* and *Ticinepomis* (Cavin et al., 2013:fig. 5; Manuelli et al., 2024:figs. 5C, 12E), and later forms such as *Megalocoelacanthus* and *Latimeria* (Dutel et al., 2012:fig. 15B; Dutel et al., 2013:fig. 1A; 2015b), suggesting a latimerioid affinity. However, it should be noted that isolated symplectic bones are not character informative and must be treated as indeterminate.

We suggest that BRSMG Ce17775 (Fig. 13F, G) is a left symplectic, a specimen previously figured as the left caudal rib of *Pachystropheus* (Storrs et al., 1996:fig. 6B), but facets for the caudal ribs are seemingly absent in *Pachystropheus* and the specimen is considerably larger than most recorded vertebrae (Quinn et al., 2024; Storrs et al., 1996). The specimen was recorded alongside symplectic BRSMG Ce17773, although it is apparently not from the same individual. Again, the bone lacks any diagnostic feature, though it is small and robust, unlike morphotype 1 (e.g., BRSMG Ce17773:fig. 13 A–C), but similarly is well-ossified. Both ends are expanded moderately with a greater expansion towards the dorsal portion of the specimen, similar to BRSMG Ce17773, yet lacks the hatchet shape seen in latimerioid coelacanths (Dutel et al., 2012:fig. 15B; Dutel et al., 2013:fig. 1A; Manuelli et al., 2024:figs. 5C, 12E). The lateral surface is smooth, and faint crenulations run dorsoventrally to the tips of the ventral end of the bone (Fig. 13G, cr). The shaft is constricted, appearing as convex on the lateral side and concave on the medial. A similar type of morphology is found amongst coelacanths, but the absence of the hatchet shape raises questions about its latimerioid affinities. It is worth noting that BRSMG Ce17775 is more or less anteroposteriorly symmetric, whereas the shaft of

FIGURE 14. Interpretative reconstruction of a large mawsoniid coelacanth alongside several juvenile individuals of the Rhaetian thalattosaur *Pachystropheus rhaeticus*, based on materials described here, and associations of fossils of the two taxa. Artist credit: Daniel Phillips.

symplectic morphotype 1 projects in a dorsoposterior direction, as in other latimerioid symplectics (Dutel et al., 2012:fig. 15B; Dutel et al., 2013:fig 1A; Manuelli et al., 2024:figs. 5C, 12E).

**Gular Region**—Gular plate: The only example of a coelacanth gular plate from the British Rhaetian, NHMUK PV UK P 73214 (Fig. 13H), was described by Hauser and Martill (2013), and we re-describe it. The specimen is an isolated, almost entirely preserved right gular plate with just a small posterior part missing, albeit the external mold of the missing portion is still visible (Hauser & Martill, 2013). The gular plate is tentatively identified as being from the right side, considering its shape. The specimen is exposed in internal view, exhibiting a gently concave inner surface. The gular plate is asymmetric, with a convexly curved lateral edge and a continually straight medial margin where the gular plates meet. Similar to many of the other coelacanth bones described here, the surface is shiny and smooth. Further, there is faint ornamentation in the center of the internal surface (Fig. 13H), as well as faint striae on the anterior. Such faint striae are seen also in mawsoniids, such as *Mawsonia gigas* (Toriño et al., 2021b:fig. 14C, D), and latimeriids, such as *Megalocoelacanthus* (Dutel et al., 2012:fig. 14C), but do not seem to be present in other genera of coelacanths, such as the Late Jurassic latimerid *Libys polypterus* (Hauser & Martill, 2013). The specimen is morphologically comparable to the gular plates of several coelacanth genera (Hauser & Martill, 2013:fig. 4), as a thin (1.2 mm) dermal bone that is loosely 'D' shaped, tapering slightly at the posterior. Unfortunately, the external ornamentation of the bone cannot be seen, which is a diagnostic feature in Cretaceous mawsoniids (e.g., *Mawsonia* and *Axelrodichthys*), typically exhibiting striae radiating from the middle point of the ossification (Fragoso et al., 2018; Toriño et al., 2021b).

## DISCUSSION

### Mistaken Identity

Coelacanth diversity peaked in the Lower–Mid Triassic, so it is surprising just how poorly examples from the British Rhaetian have been reported (Allard et al., 2015; Duffin, 1978:fig. 7; Duffin, 1999:fig. 8; Hauser & Martill, 2013; Moreau et al., 2021). Further, previous discussions have highlighted that the robust, well-ossified nature of coelacanth bones would give them a high preservation potential (Hauser & Martill, 2013; Allard et al., 2015) and yet researchers have seemingly not followed up these early leads. The isolated and often fragmentary nature of vertebrate specimens from the British Rhaetian deposits means it is difficult to identify individual ossifications and the same has been true for coelacanths from these deposits, leading to mistakes in attribution. Even once identified as a coelacanth

fossil, the exact ossification within the skeleton can be difficult to identify (e.g., Evans et al., 2024:fig. 7M).

Many registered specimens, some dating back to the late 1800s, were identified prior to the recognition of coelacanths from these deposits, resulting in misidentifications such as cranial bones of *Ceratodus* or those of an indeterminate reptile. In the first record of coelacanths from the British Rhaetian, a small, but robust quadrate from the Neptunian dyke fissure at Holwell (BRLSI unregistered specimen) is described as a phalanx of a lepidosaur or mammal in the same sentence (Duffin, 1978:fig. 7), though this was later corrected (Duffin, 1999:fig. 8). Later, coelacanth specimens were described as skull elements of the thalattosaur *Pachystropheus rhaeticus* (Quinn et al., 2024; Storrs et al., 1996), based on superficial similarities between *Pachystropheus* postcranial and coelacanth cranial fossils such as: similar preservation quality, crenulations on the surface of bones, poorly ossified articulating ends of bones that are cartilage capped, and associations of the two taxa in some instances (Quinn et al., 2024). It is also notable that many specimens, particularly those collected by the late N. Large and stored at NHMUK, have incorrect provenance, with nearly all of the specimens collected from Westbury Garden Cliff recorded as found at Blue Anchor, Somerset, for some unknown reason. Nonetheless, these misidentifications have led to long confusion, with many specimens in collections and publications misidentified (Sander et al., 2016:fig. 20G; Williams et al., 2022:fig. 10F).

## Relationships

Unfortunately, isolated coelacanth bones are not character informative for testing phylogenetic relationships. The morphological variability of particular coelacanth elements shown here can reflect some ontogenetic or sexual dimorphism, but also variability between species. Further, we note that though generally rare, where coelacanths are present in faunal assemblages, they are represented by several closely related taxa, as in the case of *Graulia* (Manuelli et al., 2024). An alternative hypothesis is that the range of morphological variation documents individual differences (polymorphism) within the population, such as in the *Mawsonia* material from the Sanfranciscana basin, Brazil (Carvalho & Maisey, 2008). Comparisons with described coelacanths indicate that many are referrable to Mawsoniidae based on characters such as the narrow "U" shaped dorsum sellae in the basisphenoids (Fig. 3; Hartung et al., 2021). Interestingly, we find few similarities between the material described here and better-known coelacanths from the Middle–Late Triassic, such as *Graulia* (Manuelli et al., 2024), and more similarities are observed with later Mesozoic forms (e.g., *Trachymetopon*, *Mawsonia*, and *Axelrodichthys*). This may suggest that our Rhaetian specimens are early occurrences of later clades, such as Mawsoniidae, with stable morphology through to the Late Cretaceous (see also Paleobiogeography below). Difficulties in establishing relationships between Early–Middle Triassic forms and later Mesozoic mawsoniids, despite well-preserved specimens, may arise from the sudden radiation of coelacanths in the Early Triassic which causes difficulties in detecting synapomorphies and resolving phylogenetic interrelationships (Manuelli et al., 2024).

## Paleoecology

The Rhaetian bone beds from which the described material originates are interpreted as products of a shallow, storm-dominated, continental shelf sea (Allington-Jones et al., 2010; Storrs, 1994; Williams et al., 2022). The south-west of England and south Wales were then marked by a complex ecosystem in which an archipelago of islands of Carboniferous limestone sat within a rising shallow sea (Lovegrove et al., 2021). The palynomorph assemblage of these deposits, at least at times, is terrestrially dominated, particularly with spores attributed to the mire plant *Lepidopteris ottonis* (Vadja et al., 2023), and when considered with other freshwater fossils, suggest wetland environments surrounding, or in close proximity to the Bristol paleo-islands (Quinn et al., 2024).

The faunal assemblage of the Westbury Formation is like that of other Late Triassic marine deposits, particularly the Norian-aged Zorzino Limestone in Italy (Tintori & Lombardo, 2018), rich in marine tetrapods, chondrichthyans, and osteichthyans (Quinn et al., 2024; Swift & Martill, 1999). The abundance of benthic invertebrates supported a range of durophages, animals with dentitions for crushing hard-shelled prey, such as the shark *Lissodus minimus* and pycnodont fishes, while placodont reptiles effectively combed inshore localities (Evans et al., 2024; Norden et al., 2015). Teeth of large predatory fishes such as *Birgeria acuminata* and *Saurichthys longidens* (Diependaal & Reumer, 2021) are common, possibly shed when eating small fishes, such as *Gyrolepis albertii*, or other marine vertebrates. Plesiosaurs and huge ichthyosaurs, though rare in the shallow marine deposits, presumably pursued larger prey in deeper water offshore, while *Pachystropheus*, an enigmatic and possibly edentulous thalattosaur, had a unique ecology within the Westbury, perhaps foraging in the muddy substrate (Quinn et al., 2024).

The paleoecology of the Rhaetian coelacanths can only be inferred from the ecology of extant and more complete extinct coelacanths (Cavin et al., 2021; Forey, 1998, 2009). The Late Triassic, and indeed the remainder of the Mesozoic, was dominated by latimerioid coelacanths (Cavin et al., 2019, 2021; Clement et al., 2024; Ferrante & Cavin, 2023; Toriño et al., 2021a). Though both share the same evolutionary traits, latimeriid coelacanths are deep-water marine taxa, while mawsoniid coelacanths seemingly thrived in brackish or freshwater environments, though there are some marine members of the clade, such as the enigmatic *Trachymetopon* (Cavin et al., 2019; Dutel et al., 2015a). Although the Westbury Formation is largely regarded as marine (Storrs, 1994), findings by Quinn et al. (2024) would suggest a brackish or freshwater environment when close to land, possibly explaining how two closely related taxa with differing ecological niches could exist within the same deposits (but the possibility that these mawsoniids were fully adapted to marine conditions cannot be discarded). This is discussed further below.

Even though determination to species level is impossible, the distribution of the coelacanth specimens and their relative frequencies across the British Rhaetian localities (Fig. 1) suggests that there were two closely related taxa with differing ecological niches. The Rhaetian marine transgression occurred from west to east in south-west Britain, meeting the coasts of north Somerset and south Wales first, as evidenced by the marine conditions of the early Rhaetian Williton Member of the Blue Anchor formation at Lilstock, Somerset (Fig. 1; Bonis et al., 2010; Durbin et al., 2024). As the transgression progressed and sea levels rose, coupled with coeval tectonics causing some basins to descend, the water in these areas was likely considerably deeper than in the east (Durbin et al., 2024; Lovegrove et al., 2021). Only one specimen attributable to Latimeriidae, BRSMG Cg3102 (Fig. 3M), was reported from north Somerset (Fig. 1), but this deep-water setting aligns with the known ecology for latimeriid coelacanths. Further, the specimen is well preserved with little abrasion, unlike terrestrial fossils seen on the slab (Quinn et al., 2024:fig. 12c), suggesting minimal transportation before deposition.

Most of the specimens come from locations to the east of the Bristol Channel where the water was shallower, with more than half (54.9%) of the sample reported as from Westbury Garden Cliff and a further 35.29% from Aust Cliff (Fig. 1). Conditions at Westbury Garden Cliff were shown to be variable,

demonstrated by the fluctuation between deep-water and shallow-water sediments, as well as horizons rich in limulid trails and bivalve burrows in sediments that indicate a shoreline environment at times of marine regression (Williams et al., 2022). Fossils of *Pachystropheus rhaeticus* are also among the most common vertebrate fossils at Westbury Garden Cliff, where they possibly took advantage of the shallow waters and abundance of benthic invertebrates at time of high oxygen inputs (Quinn et al., 2024; Williams et al., 2022). We find that coelacanth fossils occur frequently alongside specimens of *Pachystropheus* at Westbury Garden Cliff, and elements of both taxa show minimal abrasion, suggesting they are autochthonous; the two therefore may have had similar ecological preferences, foraging for food along the sea floor (Fig. 14). The coelacanths may even have preyed on the small thalattosaurs, given that their bones indicate large-sized coelacanths (possibly up to 1.5 m; see Toriño et al., 2024) in the Late Triassic (Fig. 14) comparable to *Mawsonia gigas* (Fig. 11). Although the material described occurs as isolated specimens, the numerous morphotypes of many bones in the sample hint at a complex community structure, with individuals of varying age, size, and possibly species, supported within the Rhaetian marine food web (Quinn et al., 2024:fig. 17). Their possible preference for shallow waters matches the identification of many as belonging to Mawsoniidae, a clade elsewhere reported from brackish, near-shore conditions.

### Historical European Paleobiogeography of Mawsoniidae

The historical paleobiogeography of Mawsoniidae, summarized by Toriño et al. (2022), is complex. Based on findings of the marine genus *Trachymetopon* in Early Jurassic deposits from Germany, Dutel et al. (2015a) suggested that mawsoniid coelacanths were already present in Europe prior to the Early Jurassic. Fragmentary records of Mawsoniidae were described from Rhaetian marine deposits in France and Germany, expanding their temporal range (Deesri et al., 2018; Hartung et al., 2021), and further evidence for a European origin came from the new basally branching mawsoniid *Graulia* from French Middle Triassic (Ladinian) marine deposits (Manuelli et al., 2024; see also Cavin et al., 2019). Our new fossils, although comprising isolated elements, are probably mawsoniids by comparative analysis with confirmed members of the clade (Toriño et al., 2022).

Quadrates, the first coelacanth bones from the British Rhaetian, were identified from Neptunian dyke fissures at Holwell, Somerset by Duffin (1978, 1999). The sediment in the fissure infills at Holwell was injected into active fault systems from a nearshore marine environment, as shown by the dominant fossils of *Lissodus* and *Gyrolepis* and rare placodonts, but the faunal assemblage also includes, in small proportions (usually >1%), non-marine fishes (*Pholidophorus*, *Legnonotus*, *Semionotus*) and terrestrial vertebrates, such as rhynchocephalians (*Clevosaurus* and *Diphydontosaurus*), other lepidosaurs, dinosaurs (*Thecodontosaurus*) and a possible phytosaur (Whiteside & Marshall, 2008; Whiteside et al., 2016; Weeks et al., 2025). While Hauser and Martill (2013) wrongly observed that other coelacanth material from Holwell derives from a freshwater fissure fill deposit (the deposits are Neptunian dykes), they noted elsewhere that Mesozoic coelacanths have been reported from fresh, brackish, and marine paleoenvironments (Schaeffer, 1967; Yabumoto, 2005). The specimens are abraded (Duffin, 1978:fig. 7; Duffin, 1999:fig. 8), which makes confirming affinities difficult (Hauser & Martill, 2013), but the specimens and their context are consistent with the inferred paleobiogeography of Mawsoniidae.

Coelacanth fossils identified from the British Rhaetian have predominantly been from the Westbury Formation, which is coeval with the fissure infills at Holwell (Whiteside & Marshall, 2008; Whiteside et al., 2016). British Rhaetian coelacanths are most abundant in the lower–mid Westbury Formation, but at least one specimen, the clavicle NMW2020.14G.7, can be considered as from the upper Westbury Formation, from the same horizons as one of the *Pachystropheus* specimens (Quinn et al., 2024).

The palynomorph assemblage of *Pachystropheus* bearing strata is terrestrially dominated, with abundant spores of *Ricciisporites tuberculatus*, and surprisingly few marine dinoflagellates, suggesting a coastal wetland environment proximal to the paleo-islands (Quinn et al., 2024). Similarly to the mawsoniid described from the English Late Jurassic (Toriño et al., 2022), the Rhaetian coelacanths may have lived in a shallow marine setting with occasional freshwater inputs from heavy rain on the neighboring paleo-islands. Mawsoniid coelacanths such as *Mawsonia* and *Axelrodichthys* may have been euryhaline (Barbosa et al., 2022; Cavin et al., 2021; Toriño et al., 2022). Furthermore, the bone beds of the Westbury Formation yield rare fossils of allochthonous terrestrial (dinosaurs) and freshwater (*Ceratodus*) vertebrates, often with little pre-depositional erosion, which were likely washed in during a flood or storm-surge ebb and deposited in low-energy environments (Quinn et al., 2024).

If mawsoniids were brackish/freshwater tolerant, the Rhaetian marine transgression and British Rhaetian paleoenvironment may have been key to their dispersal. Further, the Rhaetian Sea across the U.K. is shown to have been brackish, indicated by mean oxygen isotope values of less than 20% found in hybodont shark teeth from the Westbury Formation (Fischer et al., 2012; Williams et al., 2022). This aligns with the suggestion that the two main clades of Mawsoniidae, in the Triassic and Early Cretaceous, also occurred in mainly brackish and fresh waters (Cavin et al., 2019). However, if mawsoniids were euryhaline (Barbosa et al., 2022; Cavin et al., 2021; Toriño et al., 2022), this would have enabled them to colonize a broad range of environments. The mawsoniids from the Ladinian and Rhaetian of France (Deesri et al., 2018; Manuelli et al., 2024) and Rhaetian of Germany (Hartung et al., 2021) occur in marine deposits, though palynomorph analysis from deposits at Bonenburg suggest a brackish environment, at least at intervals (Gravendyck et al., 2020). It should also be noted that the German Rhaetian deposits yielding coelacanths (Bonenburg, City of Warburg, Westphalia), similarly to the British Westbury Formation, produce considerable amounts of allochthonous terrestrial and freshwater specimens (Konietzko-Meier, 2019; Sander et al., 2016; Sander & Wellnitz, 2024), and so transportation of mawsoniid remains into the marine realm is possible. In addition to the German, French Ladinian, and Rhaetian specimens, the next oldest occurrence of a European mawsoniid, *Trachymetopon* from the German Toarcian (Dutel et al., 2015a), is also from indisputably marine deposits.

Deciphering the context of mawsoniid remains in the European Middle–Late Triassic and Early Jurassic with such variability between paleoenvironmental settings is difficult, particularly where allochthonous terrestrial and freshwater fossils are abundant. One scenario is that euryhaline mawsoniids could colonize all these environments. An alternative hypothesis is that mawsoniids went through intermittent marine and brackish/freshwater phases between the Middle Triassic and Jurassic, varying in ecologies with the availability of paleoenvironments. For example, the transition from Norian-aged arid, terrestrial environments to shallow marine with the Rhaetian transgression, would have created seas and inland waterways over much of the area that is now Western Europe, and may have enabled mawsoniids to explore new ecological realms critical to their dispersal.

Though large-bodied mawsoniids, exceeding 1 m in length (Torino et al., 2024), are evidently present in the European Rhaetian, they were already widely distributed across Europe and Asia, especially if the Middle Triassic Chinese

*Luopingcoelacanthus* and *Yunnancoelacanthus* are regarded as mawsoniids (Wen et al., 2013). However, the Late Permian *Changxingia* has been proposed as a mawsoniid (Wen et al., 2013), suggesting that the origin of the group could be traced further back to Asia.

## ACKNOWLEDGMENTS

We recognize the late Nick Large for his contributions to this study; nearly all specimens featured in this study were collected by Large over 50 years. It is indeed thanks to his collecting efforts and recognition of these specimens as unique that this study is possible.

We thank C. Hildebrandt of the University of Bristol (UoB), D. Hutchinson of the Bristol City Museum and Art Gallery; A. Clark of the Museum in the Park; C. Howells of the National Museum of Wales; E. Bernard and M. Jones of the Natural History Museum; A. Smith of Wollaton Hall Natural History Museum for access to collections. Additional thanks to M. Cawthorne (UoB) and D. Hutchinson for photography guidance; F. Feneru of the Angela Marmont Centre NHMUK. We thank J. Thompson (UoB), M. Derème (UoB), M. Myerscough, and J. Bow for support with field trips—with additional thanks to Bow for his donations and local knowledge; The Peterborough Geological and Palaeontological Group, with additional thanks to T. Naylor and D. Withers, Engineering and Physical Sciences Research Council (EPSRC) for their funding of scans; μ-VIS X-ray Imaging Centre core team for scanning specimens; and H. Dutel (UoB) for support with some identifications. P. Toriño was supported by SNI_2020_1_1010231. J. Quinn thanks Prof. P. M. Sander and Dr. A. Schwermann for their invitation to LWL-Museum für Naturkunde and hospitality. M. Suhr is thanked for access to his large array of self-collected Rhaetian vertebrate material. We thank L. Cavin and an anonymous referee for their thorough and helpful reviews. We thank paleoartist D. Phillips for his detailed reconstruction of a coelacanth from the British Rhaetian.

## AUTHOR CONTRIBUTIONS

The project was supervised by MJB and DIW. JQ identified the data, analyzed them, and drafted the manuscript. ERMR found and prepared BRSMG Cg3102. PT acted as advisor and supported with identifications. All authors edited the manuscript. The paper results from the thesis submitted by J.Q. for his MSc in Palaeobiology at the University of Bristol.

## DATA AVAILABILITY STATEMENT

Data from this study is available at Morphobank (http://morphobank.org/permalink/?P5803) and Morphosource (https://www.morphosource.org/media-lists/000716642?locale=en).

## DISCLOSURE STATEMENT

No potential conflict of interest was reported by the author(s).

## ORCID

Jacob G. Quinn http://orcid.org/0009-0009-0396-6680
David I. Whiteside http://orcid.org/0000-0003-1619-747X
Pablo Toriño http://orcid.org/0000-0002-1006-9736
Michael J. Benton http://orcid.org/0000-0002-4323-1824

## SUPPLEMENTARY FILES

Supplementary File 1.xlsx: Complete roster of museum specimens studied, including previous identifications.

## LITERATURE CITED

Allard, H., Carpenter, S. C., Duffin, C. J., & Benton, M. J. (2015). Microvertebrates from the classic Rhaetian bone beds of Manor Farm Quarry, near Aust (Bristol, UK). *Proceedings of the Geologists' Association*, *126*(6), 762–776. doi:10.1016/j.pgeola.2015.09.002

Allington-Jones, L., Braddy, S. J., & Trueman, C. N. (2010). Palaeoenvironmental implications of the ichnology and geochemistry of the Westbury Formation (Rhaetian), Westbury-on-Severn, south-west England. *Palaeontology*, *53*(3), 491–506. doi:10.1111/j.1475-4983.2010.00947.x

Barbosa, R., da Silva, M. C., & Barreto, A. M. F. (2022). New records of Mawsoniidae (Actinistia) from the Romualdo Formation, Aptian-Albian of the Araripe Basin in Pernambuco state, Brazil. *Journal of South American Earth Sciences*, *113*, 103637. doi:10.1016/j.jsames.2021.103637

Batista, T. A., Bantim, R. A. M., de Lima, F. J., dos Santos Filho, E. B., & Saraiva, AÁF. (2019). New data on the coelacanth fish-fauna (Mawsoniidae) from the Late Jurassic and Early Cretaceous of Araripe Basin, Brazil. *Journal of South American Earth Sciences*, *95*, 102280. doi:10.1016/j.jsames.2019.102280

Bonis, N. R., Ruhl, M., & Kürschner, W. M. (2010). Milankovitch-scale palynological turnover across the Triassic–Jurassic transition at St. Audrie's Bay, SW UK. *Journal of the Geological Society*, *167*(5), 877–888. doi:10.1144/0016-76492009-141

Carvalho, M. S., & Maisey, J. G. (2008). New occurrence of *Mawsonia* (Sarcopterygii: Actinistia) from the Early Cretaceous of the Sanfranciscana Basin, Minas Gerais, southeastern Brazil. *Geological Society, London, Special Publications*, *295*(1), 109–144. doi:10.1144/SP295.8

Carvalho, M. S. S. D. (2002). O gênero *Mawsonia* (Sarcopterygii, Actinistia) no Cretáceo das bacias Sanfranciscana, Tucano, Araripe, Parnaíba e Sao Luiz (Doctoral dissertation).

Cavin, L., Buffetaut, E., Dutour, Y., Garcia, G., Le Loeuff, J., Mechin, A., Mechin, P., Tong, H., Tortosa, T., Turini, E., & Valentin, X. (2020). The last known freshwater coelacanths: New Late Cretaceous mawsoniid remains (Osteichthyes: Actinistia) from southern France. *PLoS ONE*, *15*(6), e0234183. doi:10.1371/journal.pone.0234183

Cavin, L., Cupello, C., Yabumoto, Y., Fragoso, L., Deesri, U., & Brito, P. M. (2019). Phylogeny and evolutionary history of mawsoniid coelacanths. *Bulletin of the Kitakyushu Museum of Natural History and Human History, Series A (Natural History)*, *17*, 3–13.

Cavin, L., Furrer, H., & Obrist, C. (2013). New coelacanth material from the Middle Triassic of eastern Switzerland, and comments on the taxic diversity of actinistans. *Swiss Journal of Geosciences*, *106*(2), 161–177. doi:10.1007/s00015-013-0143-7

Cavin, L., & Grădinaru, E. (2014). Dobrogeria aegyssensis, a new early Spathian (Early Triassic) coelacanth from north Dobrogea (Romania). *Acta Geologica Polonica*, *64*(2), 161–187. doi:10.2478/agp-2014-0010

Cavin, L., Valentin, X., & Garcia, G. (2016). A new mawsoniid coelacanth (Actinistia) from the Upper Cretaceous of Southern France. *Cretaceous Research*, *62*, 65–73.

Cavin, L., Mennecart, B., Obrist, C., Costeur, L., & Furrer, H. (2017). Heterochronic evolution explains novel body shape in a Triassic coelacanth from Switzerland. *Scientific Reports*, *7*(1), 13695. doi:10.1038/s41598-017-13796-0

Cavin, L., Tong, H., Buffetaut, E., Wongko, K., Suteethorn, V., & Deesri, U. (2023). The first fossil coelacanth from Thailand. *Diversity*, *15*(2), 286. doi:10.3390/d15020286

Cavin, L., Toriño, P., Van Vranken, N., Carter, B., Polcyn, M. J., & Winkler, D. (2021). The first late cretaceous mawsoniid coelacanth (Sarcopterygii: Actinistia) from North America: Evidence of a lineage of extinct 'living fossils'. *PLoS ONE*, *16*(11), e0259292. doi:10.1371/journal.pone.0259292

Clement, A. M., Cloutier, R., Lee, M. S., King, B., Vanhaesebroucke, O., Bradshaw, C. J., Dutel, H., Trinajstic, K., & Long, J. A. (2024). A Late Devonian coelacanth reconfigures actinistian phylogeny, disparity, and evolutionary dynamics. *Nature Communications*, *15*(1), 7529. doi:10.1038/s41467-024-51238-4

Cloutier, R. (1991a). Interrelationships of Palaeozoic actinistians: patterns and trends. In M. M. Chan, Y. H. Li, & G. R. Zhang (Eds.),

*Early Vertebrates and Related Problems of Evolutionary Biology* (pp. 379–428). Science Press.

Cloutier, R. (1991b). Patterns, trends, and rates of evolution within the Actinistia. In J. A. Musick, M. N. Bruton, & E. K. Balon (Eds.), *The Biology of* Latimeria chalumnae *and Evolution of Coelacanths* (pp. 23–58). Kluwer.

Cloutier, R., & Forey, P. L. (1991). Diversity of extinct and living actinistian fishes (Sarcopterygii). In J. A. Musick, M. N. Bruton, & E. K. Balon (Eds.), *The Biology of* Latimeria chalumnae *and Evolution of Coelacanths* (pp. 59–74). Kluwer.

Cope, E. D. (1871). Contribution to the ichthyology of the Lesser Antilles. *Transactions of the American Philosophical Society*, *14*(3), 445–483. doi:10.2307/1005256

Cupello, C., Batista, T. A., Fragoso, L. G., & Brito, P. M. (2016). Mawsoniid remains (Sarcopterygii: Actinistia) from the lacustrine Missão Velha Formation (Lower Cretaceous) of the Araripe Basin, North-east Brazil. *Cretaceous Research*, *65*, 10–16. doi:10.1016/j.cretres.2016.04.009

Deesri, U., Cavin, L., Amiot, R., Bardet, N., Buffetaut, E., Cuny, G., Giner, S., Martin, J. E., & Suan, G. (2018). A mawsoniid coelacanth (Sarcopterygii: Actinistia) from the Rhaetian (Upper Triassic) of the Peygros quarry, Le Thoronet (Var, southeastern France). *Geological Magazine*, *155*(1), 187–192. doi:10.1017/S0016756817000619

Diependaal, H. J., & Reumer, J. W. (2021). Note on the Rhaetian fish fauna from a subrosion pipe in Winterswijk (the Netherlands), with a discussion on the validity of the genus *Severnichthys* Storrs, 1994. *Netherlands Journal of Geosciences*, *100*, e9. doi:10.1017/njg.2021.5

Duffin, C. J. (1978). The Bath geological collections: the importance of certain vertebrate fossils collected by Charles Moore: an attempt at a scientific perspective. *Geological Curator*, *2*(2), 59–67. doi:10.55468/GC1055

Duffin, C. J. (1999). Fish. In A. Swift, & D. M. Martill (Eds.), *Fossils of the Rhaetian Penarth Group* (pp. 191–222). Palaeontological Association.

Durbin, O. L., Duffin, C. J., Hildebrandt, C., & Benton, M. J. (2024). Onset of the Rhaetian Transgression in deep waters at Lilstock, North Somerset: Microvertebrate faunas. *Proceedings of the Geologists' Association*, *135*(2), 181–195. doi:10.1016/j.pgeola.2024.02.001

Dutel, H., Herbin, M., & Clément, G. (2015a). First occurrence of a mawsoniid coelacanth in the Early Jurassic of Europe. *Journal of Vertebrate Paleontology*, *35*(3), e929581. doi:10.1080/02724634.2014.929581

Dutel, H., Herrel, A., Clément, G., & Herbin, M. (2015b). Redescription of the hyoid apparatus and associated musculature in the extant coelacanth *Latimeria chalumnae*: functional implications for feeding. *The Anatomical Record*, *298*(3), 579–601. doi:10.1002/ar.23103

Dutel, H., Herrel, A., Clément, G., & Herbin, M. (2013). A reevaluation of the anatomy of the jaw-closing system in the extant coelacanth *Latimeria chalumnae*. *Naturwissenschaften*, *100*(11), 1007–1022. doi:10.1007/s00114-013-1104-8

Dutel, H., Maisey, J. G., Schwimmer, D. R., Janvier, P., Herbin, M., & Clément, G. (2012). The giant Cretaceous coelacanth (Actinistia, Sarcopterygii) *Megalocoelacanthus dobiei* Schwimmer, Stewart & Williams, 1994, and its bearing on Latimerioidei interrelationships. *PLoS ONE*, *7*(11), e49911. doi:10.1371/journal.pone.0049911

Dutel, H., Pennetier, E., & Pennetier, G. (2014). A giant marine coelacanth from the Jurassic of Normandy, France. *Journal of Vertebrate Paleontology*, *34*(5), 1239–1242. http://doi.org/10.1080/02724634.2014.838176

Dutel, H., Galland, M., Tafforeau, P., Long, J. A., Fagan, M. J., Janvier, P., Herrel, A., Santin, M. D., Clément, G., & Herbin, M. (2019). Neurocranial development of the coelacanth and the evolution of the sarcopterygian head. *Nature*, *569*(7757), 556–559. doi:10.1038/s41586-019-1117-3

Evans, O., Duffin, C. J., Hildebrandt, C., & Benton, M. J. (2024). Microvertebrates from the basal Rhaetian Bone Bed (Late Triassic) at Lavernock, South Wales. *Proceedings of the Geologists' Association*, *135*(3), 321–334. doi:10.1016/j.pgeola.2024.05.001

Ferrante, C., Furrer, H., Martini, R., & Cavi, L. (2023). Revision of the Middle Triassic coelacanth *Ticinepomis* Rieppel 1980 (Actinistia, Latimeriidae) with paleobiological and paleoecological considerations. *Swiss Journal of Palaeontology*, *142*(1), 18. https://doi.org/10.1186/s13358-023-00276-4

Ferrante, C., & Cavin, L. (2023). Early Mesozoic burst of morphological disparity in the slow-evolving coelacanth fish lineage. *Scientific Reports*, *13*(1), 11356. doi:10.1038/s41598-023-37849-9

Fischer, J., Voigt, S., Franz, M., Schneider, J. W., Joachimski, M. M., Tichomirowa, M., Götze, J., & Furrer, H. (2012). Palaeoenvironments of the late Triassic Rhaetian Sea: implications from oxygen and strontium isotopes of hybodont shark teeth. *Palaeogeography, Palaeoclimatology, Palaeoecology*, *353-355*, 60–72. doi:10.1016/j.palaeo.2012.07.002

Forey, P. L. (1998). *History of the Coelacanth Fishes*. Springer Science & Business Media.

Forey, P. L. (2009). *Coelacanth: Portrait of a Living Fossil*. Forrest Text.

Forey, P., & Young, V. (1985). Acanthodian and coelacanth fish from the Dinantian of Foulden, Berwickshire, Scotland. *Transactions of the Royal Society of Edinburgh: Earth Sciences*, *76*(1), 53–59. doi:10.1017/S0263593300010300

Forey, P. L. (1991). *Latimeria chalumnae* and its pedigree. In J. A. Musick, M. N. Bruton, & E. K. Balon (Eds.), *The Biology of* Latimeria chalumnae *and Evolution of Coelacanths* (pp. 75–98). Kluwer.

Fragoso, L. G. C., Brito, P., & Yabumoto, Y. (2019). *Axelrodichthys araripensis* Maisey, 1986 revisited. *Historical Biology*, *31*, 1350–1372.

Friedman, M., & Coates, M. I. (2006). A newly recognized fossil coelacanth highlights the early morphological diversification of the clade. *Proceedings of the Royal Society, B*, *273*(1583), 245–250. doi:10.1098/rspb.2005.3316

Gravendyck, J., Schobben, M., Bachelier, J. B., & Kürschner, W. M. (2020). Macroecological patterns of the terrestrial vegetation history during the end-Triassic biotic crisis in the central European Basin: a palynological study of the Bonenburg section (NW-Germany) and its supraregional implications. *Global and Planetary Change*, *194*, 103286. doi:10.1016/j.gloplacha.2020.103286

Hartung, J., Sander, P. M., Friedman, M., & Wintrich, T. (2021). First record of mawsoniid coelacanths (Actinistia, Sarcopterygii) from the marine Rhaetian (Upper Triassic) of Bonenburg, Germany. *Journal of Vertebrate Paleontology*, *41*(2), e1931258. doi:10.1080/02724634.2021.1931258

Hauser, L. M., & Martill, D. M. (2013). Evidence for coelacanths in the Late Triassic (Rhaetian) of England. *Proceedings of the Geologists' Association*, *124*(6), 982–987. doi:10.1016/j.pgeola.2013.07.005

Huxley, T. H. (1861). Preliminary essay upon the systematic arrangement of the fishes of the Devonian epoch. *Memories of the Geological Survey of the United Kingdom*, *10*, 1–40.

Hodges, P. (2021). A new ammonite from the Penarth Group, South Wales and the base of the Jurassic System in SW Britain. *Geological Magazine*, *158*(6), 1109–1114.

Hounslow, M. W., & Ruffell, A. H. (2006). Triassic: seasonal rivers, dusty deserts and saline lakes. In Brenchley, P.J., Rawson, P.F. (Eds.), *The Geology of England and Wales*. Geological Society of London, London.

Ivimey-Cook, H. (1974). *The Permian and Triassic deposits of Wales*. In T. R. Owen (Ed.), *The Upper Palaeozoic and Post-Palaeozoic rocks of Wales* (pp. 295–321). University of Wales Press.

Konietzko-Meier, D., Werner, J. D., Wintrich, T., & Sander, M. P. (2019). A large temnospondyl humerus from the Rhaetian (Late Triassic) of Bonenburg (Westphalia, Germany) and its implications for temnospondyl extinction. *Journal of Iberian Geology*, *45*(2), 287–300. doi:10.1007/s41513-018-0092-0

Larkin, N. R., Duffin, C. J., Dey, S., Stukins, S., & Falkingham, P. (2020). The first tetrapod track recorded from the Rhaetian in the British Isles. *Proceedings of the Geologists' Association*, *131*(6), 722–729. doi:10.1016/j.pgeola.2020.07.012

Lovegrove, J., Newell, A. J., Whiteside, D. I., & Benton, M. J. (2021). Testing the relationship between marine transgression and evolving island palaeogeography using 3D GIS: an example from the Late Triassic of SW England. *Journal of the Geological Society*, *178*(3), jgs2020–158. doi:10.1144/jgs2020-158

Maisey, J. G. (1986). Coelacanths from the Lower Cretaceous of Brazil. *American Museum Novitates*, *2866*, 1–30.

Mansuit, R., Clément, G., Herrel, A., Dutel, H., Tafforeau, P., Santin, M. D., & Herbin, M. (2020). Development and growth of the pectoral girdle and fin skeleton in the extant coelacanth *Latimeria chalumnae*. *Journal of Anatomy*, *236*(3), 493–509. doi:10.1111/joa.13115

Manuelli, L., Mondéjar-Fernández, J., Dollman, K., Jakata, K., & Cavin, L. (2024). The most detailed anatomical reconstruction of a Mesozoic coelacanth. *PLoS ONE*, *19*(11), e0312026. https://doi.org/10.1371/journal.pone.0312026

Millott, J.-P., & Anthony, J. (1958). *Anatomie de* Latimeria chalumnae. Tome I: Squelette, Muscles et Formations de Soutien. C.N.R.S.

Millott, J.-P., & Anthony, J. (1965). *Anatomie de* Latimeria chalumnae. Tome II: Système Nerveux et Organes des Sens. C.N.R.S.

Moreau, M., Duffin, C. J., Hildebrandt, C., Hutchinson, D., Parker, A., Carpenter, S., & Benton, M. J. (2021). Microvertebrates from the Rhaetian basal bone bed of Saltford, near Bath, SW England. *Proceedings of the Geologists' Association*, *132*(2), 174–187. doi:10.1016/j.pgeola.2020.11.003

Norden, K. K., Duffin, C. J., & Benton, M. J. (2015). A marine vertebrate fauna from the Late Triassic of Somerset, and a review of British placodonts. *Proceedings of the Geologists' Association*, *126*(4-5), 564–581. doi:10.1016/j.pgeola.2015.07.001

Object Research Systems (ORS). (2020). *Dragonfly 2020.2 [Computer software]*. Object Research Systems Inc. http://www.theobjects.com/dragonfly.

Quinn, J. G., Matheau-Raven, E. R., Whiteside, D. I., Marshall, J. E., Hutchinson, D. J., & Benton, M. J. (2024). The relationships and paleoecology of *Pachystropheus rhaeticus*, an enigmatic latest Triassic marine reptile (Diapsida: Thalattosauria). *Journal of Vertebrate Paleontology*, *43*(6), e2350408. doi:10.1080/02724634.2024.2350408

Robinson, P. L. (1957). The Mesozoic fissures of the Bristol Channel area and their vertebrate faunas. *Journal of the Linnean Society of London, Zoology*, *43*(291), 260–282. doi:10.1111/j.1096-3642.1957.tb01553.x

Romer, A. S. (1955). Herpetichthyes, Amphibioidei, Choanichthyes or Sarcopterygii? *Nature*, *176*(4472), 126–126. doi:10.1038/176126a0

Sander, P. M., & Wellnitz, P. W. (2024). A phytosaur osteoderm from a late middle Rhaetian bone bed of Bonenburg (North Rhine-Westphalia, Germany): Implications for phytosaur extinction. *Fossil Record*, *27*(1), 147–158. doi:10.3897/fr.27.e114601

Sander, P. M., Wintrich, T., Schwermann, A. H., & Kindlimann, R. (2016). Die paläontologische Grabung in der Rhät-Lias-Tongrube der Fa. Lücking bei Warburg-Bonenburg (Kr. Höxter) im Frühjahr 2015. Geologie und Paläontologie in Westfalen, 88, 11–37.

Schaeffer, B. (1952). Rates of evolution in the coelacanth and dipnoan fishes. *Evolution*, *6*(1), 101–111. doi:10.2307/2405507

Schaeffer, B. (1967). Osteichthyan vertebrae. *Journal of the Linnean Society of London, Zoology*, *47*(311), 185–195. doi:10.1111/j.1096-3642.1967.tb01402.x

Schaeffer, B., & Gregory, J. T. (1961). Coelacanth fishes from the continental Triassic of the western United States. *American Museum Novitates*, *2036*, 1–18.

Schultze, H. P. (1993). Osteichthyes: Sarcopterygii. In M. J. Benton (Ed.), *The Fossil Record 2* (pp. 657–663). Chapman and Hall.

Schultze, H. P., Fuchs, D., Giersch, S., Ifrim, C., & Stinnesbeck, W. (2010). *Palaeoctopus pelagicus* from the Turonian of Mexico reinterpreted as a coelacanth (Sarcopterygian) gular plate. *Palaeontology*, *53*(3), 689–694. doi:10.1111/j.1475-4983.2010.00943.x

Smith, J. (1940). A living coelacanthid fish from South Africa. *Transactions of the Royal Society of South Africa*, *28*(1), 1–106. doi:10.1080/00359194009519797

Stensiö, E. A. (1921). *Triassic Fishes from Spitzbergen* (pp. 307). A. Holzhausen.

Storrs, G., Gower, D., & Large, N. (1996). The diapsid reptile, *Pachystropheus rhaeticus*, a probable choristodere from the Rhaetian of Europe. *Palaeontology*, *39*, 323–349.

Storrs, G. W. (1994). Fossil vertebrate faunas of the British Rhaetian (latest Triassic). *Zoological Journal of the Linnean Society*, *112*(1-2), 217–259. doi:10.1111/j.1096-3642.1994.tb00319.x

Suan, G., Föllmi, K. B., Adatte, T., Bomou, B., Spangenberg, J. E., & Schoorbtugge, B. V. D. (2012). Major environmental change and bonebed genesis prior to the Triassic–Jurassic mass extinction. *Journal of the Geological Society*, *169*(2), 191–200. doi:10.1144/0016-76492011-045

Swift, A., & Martill, D. M. (1999). *Fossils of the Rhaetian Penarth Group*. Palaeontological Association.

Tintori, A., & Lombardo, C. (2018). The Zorzino Limestone actinopterygian fauna from the Late Triassic (Norian) of the southern Alps. In L. H. Tanner (Ed.), *The Late Triassic World: Earth in a Time of Transition* (pp. 315–350). Springer.

Toriño, P., Dutel, H., Soto, M., Norbis, W., Ezquerra, V., & Perea, D. (2024). Reconstructing an ancient fish: Three-dimensional skeletal restoration of the head of *Mawsonia* (Sarcopterygii, Actinistia) using CT scan, and an adjusted model for body size estimation in fossil coelacanths. *Journal of Anatomy*, *245*(3), 467–489. doi:10.1111/joa.14054

Toriño, P., Gausden, S. F., Etches, S., Rankin, K., Marshall, J. E., & Gostling, N. J. (2022). An enigmatic large mawsoniid coelacanth (Sarcopterygii, Actinistia) from the Upper Jurassic Kimmeridge Clay Formation of England. *Journal of Vertebrate Paleontology*, *42*(1), e2125813. doi:10.1080/02724634.2022.2125813

Toriño, P., Soto, M., & Perea, D. (2021a). A comprehensive phylogenetic analysis of coelacanth fishes (Sarcopterygii, Actinistia) with comments on the composition of the Mawsoniidae and Latimeriidae: Evaluating old and new methodological challenges and constraints. *Historical Biology*, *33*(12), 3423–3443. doi:10.1080/08912963.2020.1867982

Toriño, P., Soto, M., Perea, D., & de Carvalho, M. S. S. (2021b). New findings of the coelacanth *Mawsonia* Woodward (Actinistia, Latimerioidei) from the Late Jurassic–Early Cretaceous of Uruguay: Novel anatomical and taxonomic considerations and an emended diagnosis for the genus. *Journal of South American Earth Sciences*, *107*, 103054. doi:10.1016/j.jsames.2020.103054

Vajda, V., McLoughlin, S., Slater, S. M., Gustafsson, O., & Rasmusson, A. G. (2023). The 'seed-fern' *Lepidopteris* mass-produced the abnormal pollen *Ricciisporites* during the end-Triassic biotic crisis. *Palaeogeography, Palaeoclimatology, Palaeoecology*, *627*, 111723. doi:10.1016/j.palaeo.2023.111723

Wall, G. R., & Jenkyns, H. C. (2004). The age, origin and tectonic significance of Mesozoic sediment-filled fissures in the Mendip Hills (SW England): implications for extension models and Jurassic sea-level curve. *Geological Magazine*, *141*(4), 471–504. doi:10.1017/S0016756804009185

Warrington, G. (2008). The St Audrie's Bay-Doniford Bay section, Somerset, England: updated proposal for a candidate Global Stratotype Section and Point for the base of the Hettangian Stage, and of the Jurassic System. *International Subcommission on Jurassic Stratigraphy Newsletter*, *35*, 2–66.

Watson, D. (1921). XXIX. On the coelacanth fish. *Journal of Natural History*, *8*(45), 320–337. doi:10.1080/00222932108632589

Weeks, O. J., Cooper, R. B., Whiteside, D. I., Duffin, C. J., Copp, C., Hildebrandt, C., Hutchinson, D., & Benton, M. J. (2025). Microvertebrates from a Rhaetian neptunian dyke at Holwell, Somerset: dating the fissures. *Proceedings of the Geologists' Association*, *101112*), doi.org/10.1016j.pgeola.2025.101112

Wen, W., Zhang, Q. Y., Hu, S. X., Benton, M. J., Zhou, C. Y., Xie, T., Huang, J.-Y., & Chen, Z. Q. (2013). Coelacanths from the Middle Triassic Luoping Biota, Yunnan, South China, with the earliest evidence of ovoviviparity. *Acta Palaeontologica Polonica*, *58*, 175–193. doi: 10.4202/app.2011.0066

Whiteside, D. I., & Duffin, C. J. (2017). Late Triassic terrestrial microvertebrates from Charles Moore's 'Microlestes' quarry, Holwell, Somerset, UK. *Zoological Journal of the Linnean Society*, *179*(3), 677–705. doi:10.1111/zoj.12458

Whiteside, D. I., & Marshall, J. E. (2008). The age, fauna and palaeoenvironment of the Late Triassic fissure deposits of Tytherington, South Gloucestershire, U.K. *Geological Magazine*, *145*(1), 105–147. doi:10.1017/S0016756807003925

Whiteside, D. I., Duffin, C. J., Gill, P. G., Marshall, J. E. A., & Benton, M. J. (2016). The Late Triassic and Early Jurassic fissure faunas from Bristol and South Wales: stratigraphy and setting. *Palaeontologia Polonica*, *67*, 257–287.

Williams, H., Duffin, C. J., Hildebrandt, C., Parker, A., Hutchinson, D., & Benton, M. J. (2022). Microvertebrates from the Rhaetian bone beds at Westbury Garden Cliff, near Gloucester, UK. *Proceedings of the Geologists' Association*, *133*(2), 119–136. doi:10.1016/j.pgeola.2022.01.002

Yabumoto, Y. (2008). A new Mesozoic coelacanth from Brazil (Sarcopterygii, Actinistia). *Paleontological Research*, *12*(4), 329–343. doi:10.2517/prpsj.12.329

Yabumoto, Y., & Uycno, T. (2005). New materials of a Cretaceous coelacanth, *Mawsonia lavocati* Tabaste from Morocco. *Bulletin of the National Science Museum, Tokyo, Series C*, *31*, 39–49.

Zavialova, N. (2024). Comment on "The 'seed-fern' *Lepidopteris* mass-produced the abnormal pollen *Ricciisporites* during the end-Triassic biotic crisis" by V. Vajda, S. McLoughlin, S. M. Slater, O. Gustafsson, and A. G Rasmussen. [*Palaeogeography, Palaeoclimatology, Palaeoecology*, 627 (2023), 111, 723]. *Review of Palaeobotany and Palynology*, *322*, 105065. doi:10.1016/j.revpalbo.2024.105065

Handling Editor: Juan Liu.